Table 1. Patient Characteristics and *IL28B* Genotype

	IL28B Major*	*IL28B* Minor†	*P*-value‡
Patients, n	54	34	
Age (SD), year	58.8 (10.0)	59.1 (10.3)	0.918§
Sex, n (%)			0.051‖
Male	13 (24.1)	15 (44.1)	
Female	41 (75.9)	19 (55.9)	
BMI (SD), kg/m^2	22.7 (3.5)	23.5 (3.6)	0.193§
ALT (SD), IU/L	61.3 (50.7)	62.4 (44.7)	0.962§
γ-GTP (SD), IU/L	36.7 (25.9)	57.3 (52.4)	0.010§
LDL-cholesterol (SD), mg/dL	103.3 (29.8)	91.8 (26.9)	0.067§
Hemoglobin (SD), g/dL	14.1 (1.4)	14.4 (1.3)	0.186§
Platelet count (SD), $\times 10^3$3/μL	161 (6.4)	163 (4.4)	0.489§
Fibrosis stage, n (%)			0.532‖
F1, 2	38 (70.4)	26 (76.5)	
F3, 4	16 (29.6)	8 (23.5)	
Viral load (SD), $\times 10^{63}$ IU/mL	1.7 (1.4)	1.9 (2.0)	0.788§
%HCV core 70 & 91 a.a. double mutation¶	8.9	43.5	0.001‖
%ISDR wild**	43.5	51.7	0.486‖
Viral response, n (%)			<0.001‖
SVR	17 (31.5)	13 (38.2)	
TVR	26 (48.1)	3 (8.8)	
NVR	11 (20.4)	18 (52.9)	

Unless otherwise indicated, data are given as mean (SD).

*rs8099917 TT and rs12979860 CC.

†rs8099917 TG and rs12979860 CT.

BMI, body mass index; ALT, alanine aminotransferase; γ-GTP, γ-glutamyl transpeptidase; LDL-C, low-density lipoprotein cholesterol; HCV, hepatitis C virus; ISDR, interferon sensitivity determining region; SVR, sustained virological response; TVR, transient virological response; NVR, nonvirological response.

‡Comparison between *IL28B* major and minor genotypes.

§Mann-Whitney *U* test.

‖Chi-square test.

¶HCV core mutation was determined in 68 patients.

**ISDR was determined in 75 patients.

the therapy. After extraction of total RNA from liver biopsy specimens, the messenger RNA (mRNA) expression of the positive and negative cytoplasmic viral sensor (*RIG-I, MDA5*, and *LGP2*), the adaptor molecule (*IPS-1*), the related ubiquitin E3-ligase (*RNF125*), the modulators of these molecules (*ISG15* and *USP18*), and *IFNλ* (*IL28A/B*) was quantified by real-time quantitative polymerase chain reaction (PCR) using target gene-specific primers. In brief, total RNA was extracted by the acid-guanidinium-phenol-chloroform method using Isogen reagent (Nippon Gene, Toyama, Japan) from the liver biopsy specimen, which was 0.2-0.4 cm in length and 13G in diameter. Complementary DNA (cDNA) was transcribed from 2 μg of total RNA template in a 140-μL reaction mixture using the SYBR RT-PCR Kit (Takara Bio, Otsu, Japan) with random hexamer. Real-time quantitative PCR was performed using Smart Cycler version II (Takara Bio) with the SYBR RT-PCR Kit (Takara Bio) according to the manufacturer's instructions. Assays were performed in duplicate and the expression levels of target genes were normalized to the expressions of glyceraldehyde-3-phosphate dehydrogenase (*GAPDH*) gene and hydroxymethylbilane synthase (*HMBS*), an enzyme that is stable in the liver, as quantified using real-time quantitative PCR as internal controls. For accurate normalization, a set of two housekeeping genes was used in the present study. Sequences of the primer sets were as follows: *RIG-I*, 5′-AAAGCATGCA TGGTGTTCCAGA-3′, 5′-TCATTCGTGCATGCTC ACTGATAA-3′; *MDA5*, 5′-ACATAACAGCAACATG GGCAGTG-3′, 5′-TTTGGTAAGGCCTGAGCTGG AG-3′; *LGP2*, 5′-ACAGCCTTGCAAACAGTACAAC CTC-3′, 5′-GTCCCAAATTTCCGGCTCAAC-3′; *IPS-1*, 5′-GGTGCCATCCAAAGTGCCTACTA-3′, 5′-CAGC ACGCCAGGCTTACTCA-3′; *RNF125*, 5′-AGGGCA CATATTCGGACTTGTCA-3′, 5′-CGGGTATTAAAC GGCAAAGTGG-3′; *ISG15*, 5′-AGCGAACTCATCT TTGCCAGTACA-3′, 5′-CAGCTCTGACACCGACA TGGA-3′; *USP18*, 5′-TGGTTCTGCTTCAATGACT CCAATA-3′, 5′-TTTGGGCATTTCCATTAGCACT C-3′; *IFNλ*: 5′-CAGCTGCAGGTGAGGGA-3′, 5′-G GTGGCCTCCAGAACCTT-3′; *GAPDH*, 5′-GCACC GTCAAGGCTGAGAAC-3′, 5′-ATGGTGGTGAAGA CGCCAGT-3′; *HMBS*, 5′-AAGCGGAGCCATGTCT GGTAAC-3′, 5′-GTACCCACGCGAATCACTCTCA-3′.

Genotyping for* IL28B *(rs8099917 and rs12979860) Polymorphism. Genetic polymorphism in a tagged SNP located near the *IL28B* gene (rs8099917 and rs12979860) was determined by direct sequencing of PCR-amplified DNA. In brief, after extraction from whole blood samples, genomic DNA was amplified by PCR. Sequences of the primer sets were: rs8099917, 5′-ATCCTCCTCTCATCCCTCA TC-3′, 5′-GGTATCAACCCCACCTCAAAT-3′; rs129 79860, 5′-GGACGAGAGGGCGTTAGAG-3′, 5′-AG GGACCGCTACGTAAGTCAC-3′.

Both strands of the PCR products were sequenced by the dye terminator method using BigDye Terminator v3.1 Cycle Sequencing Kit (Applied Biosystems, Chiba, Japan); nucleotide sequences were determined by a capillary DNA sequencer ABI3730xl (Applied Biosystems). Homozygosity (rs8099917 GG and rs12979860 TT) or heterozygosity (rs8099917 TG and rs12979860 CT) of the minor sequence was defined as having the *IL28B* minor allele, whereas homozygosity for the major sequence (rs8099917 TT and rs12979860 CC) was defined as having the *IL28B* major allele.

Western Blotting. Western blotting was performed using samples from 14 patients (six from *IL28B* major patients and eight from *IL28B* minor patients) as described.[19] In brief, liver biopsy specimens of

approximately 10 mg were homogenized in 100 μL of Complete Lysis-M (Roche Applied Science, Penzberg, Germany). Next, 30 μg of protein was separated by NuPAGE 4%-12% Bis-Tris gels (Invitrogen, Carlsbad, CA) and blotted on polyvinylidene difluoride membranes. The membranes were immunoblotted with anti-RIG-I (Cell Signaling Technology, Danvers, MA) or anti-IPS-1 (Enzo Life Science, Farmingdale, NY), followed by anti-β-actin (Sigma Aldrich, St. Louis, MO). After immunoblotting with horseradish peroxidase-conjugated secondary antibody, signals were detected by chemiluminescence (BM Chemiluminescence Blotting Substrate, Roche Applied Science, Mannheim, Germany). Optical densitometry was performed using ImageJ software (NIH, Bethesda, MD). Naive Huh7 cells were used for a positive control for full-length IPS-1, and cells transfected with HCV-1b subgenomic replicon[20] were used for a positive control for cleaved IPS-1.

Definitions of Response to Therapy. A patient negative for serum HCV-RNA during the first 6 months after completing PEG-IFNα-2b/RBV combination therapy was defined as a sustained viral responder (SVR), and a patient for whom HCV-RNA became negative at the end of therapy and reappeared after completion of therapy was defined as a transient virological responder (TVR). A patient for whom HCV-RNA became negative at the end of therapy (SVR + TVR) was defined as a virological responder (VR). A patient whose HCV-RNA did not become negative during the course of therapy was defined as an NVR. HCV-RNA was determined by TaqMan HCV assay (Roche Molecular Diagnostics).

Statistical Analysis. Categorical data were compared using the chi-square test and Fisher's exact test. Distributions of continuous variables were analyzed by the Mann-Whitney *U* test for two groups. All tests of significance were two-tailed and $P < 0.05$ was considered statistically significant.

Results

Patient Characteristics and* IL28B *Genotype. Table 1 shows patient characteristics according to *IL28B* genotype. SNPs at rs8099917 and rs12979860 were 100% identical; 54 patients were identified as having the major alleles (rs8099917 TT/rs12979860 CC; *IL28B* major patients) and the remaining 34 had the minor alleles (rs8099917 TG/rs12979860 CT; *IL28B* minor patients). Patients having a minor homozygote (rs8099917 GG or rs12979860 TT) were not found in this study, which is consistent with a recent report of the rarity of a minor homozygote in Japanese patients.[3] *IL28B* minor patients were significantly associated with a higher γ-glutamyl transpeptidase (γ-GTP) level and higher frequency of mutations at amino acid positions 70 and 91 of the HCV core region (glutamine or histidine mutation at amino acid position 70; methionine mutation at amino acid position 91). NVR rate was significantly higher in *IL28B* minor patients than in *IL28B* major patients.

Gene Expression Involving Innate Immunity and* IFNλ *in the Liver. Hepatic expression levels of cytoplasmic viral sensors (*RIG-I, MDA5,* and *LGP2*) were significantly higher in *IL28B* minor patients than in *IL28B* major patients (Fig. 1). Similarly, expressions of *ISG15* and *USP18* were significantly higher in *IL28B* minor patients than in *IL28B* major patients (Fig. 1). In contrast, the hepatic expression of the adaptor molecule (*IPS-1*) was significantly lower in *IL28B* minor patients than that in *IL28B* major patients (Fig. 1). Hepatic expression of *RNF125* was similar among *IL28B* genotypes (Fig. 1). *IFNλ (IL28A/B)* expression was higher in *IL28B* minor patients, but not statistically significant (Fig. 1). Because expression of *RIG-I* and *IPS-1* were negatively correlated, the expression ratio of *RIG-I/IPS-1* in *IL28B* minor patients was significantly higher than in *IL28B* major patients (Fig. 1).

Next, to assess the relationship between baseline hepatic gene expression and treatment efficacy, we compared levels of gene expression involving innate immunity and *IFNλ* based on the final virological response (Fig. 2). Overall, hepatic expressions of cytoplasmic viral sensors and the ISG15/USP18 system in NVR patients were significantly higher than those in VR patients. In a similar but opposite manner, hepatic expressions of *IPS-1* and *RNF125* in NVR patients were significantly lower than that in VR patients, and the expression of *IFNδ* was higher in NVR patients, but the differences were not statistically significant. Expression ratio of *RIG-I/IPS-1* was significantly higher in NVR patients than that in VR patients.

Because hepatic expressions of the RIG-I/IPS-1 and ISG15/USP18 systems were significantly related both to *IL28B* minor and NVR patients, *RIG-I* and *ISG15* expression levels and the *RIG-I/IPS-1* ratio between VR and NVR patients were further stratified by *IL28B* genotype (Fig. 3). Even in the subgroup of *IL28B* minor patients, the expressions of *RIG-I* and *ISG15* were significantly higher in NVR patients than those in VR patients. Similar tendencies were observed in a subgroup of *IL28B* major patients, in whom the *RIG-I/IPS-1* expression ratio was significantly higher in

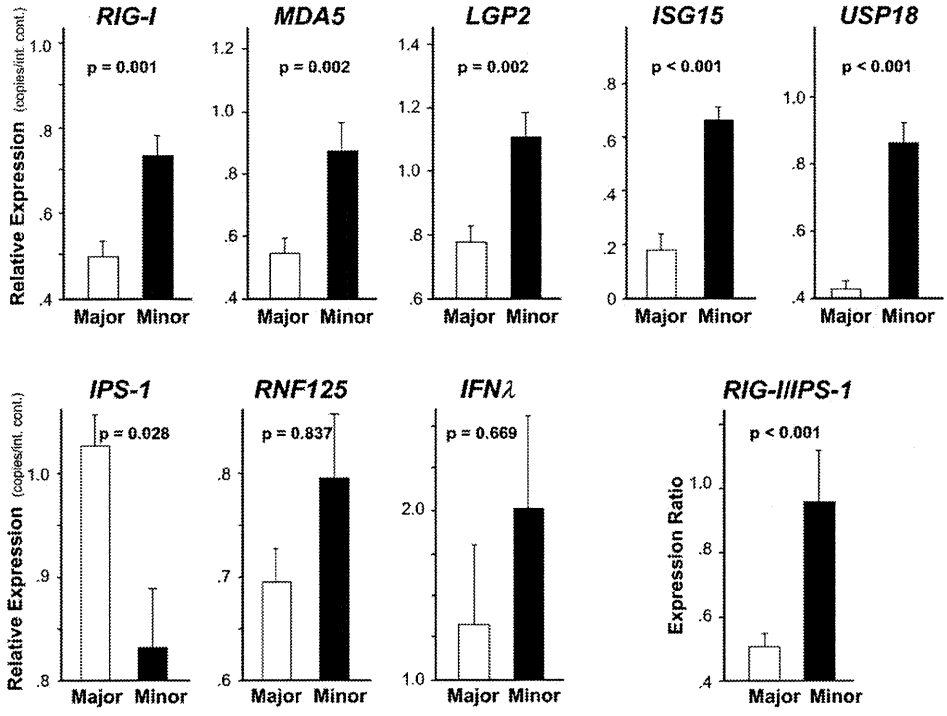

Fig. 1. Comparison of hepatic gene expression levels between *IL28B* major (rs8099917 TT/rs12979860 CC, n = 54) and *IL28B* minor patients (rs8099917 TG/rs12979860 CT, n = 34). Expression levels of cytoplasmic viral sensors (*RIG-I*, *MDA5*, and *LGP2*), modulators (*ISG15* and *USP18*), an adaptor (*IPS-1*), negative regulators (*RNF125*) and *IFNλ*, and expression ratio of the *RIG-I/IPS-1* are shown. Error bars indicate standard error. The *P*-values were determined by the Mann-Whitney *U* test.

NVR patients than in VR patients. However, in patients of the same virological response subgroup, *RIG-I* and *ISG15* expression levels and *RIG-I/IPS-1* ratio were higher in *IL28B* minor patients, and the difference in *ISG15* expression in subgroup of VR and NVR patients and that in *RIG-I/IPS-1* ratio in subgroup of VR patients was statistically significant between *IL28B* genotypes (Fig. 3).

Receiver Operator Characteristic (ROC) Analysis. To determine the usefulness of these gene quantifications and *IL28B* genotyping as predictors of NVR, an ROC analysis was conducted (Fig. 4A). The area under the ROC curve for *RIG-I* and *ISG15* expressions and *RIG-I/IPS-1* expression ratio was 0.712, 0.782, and 0.732, respectively, suggesting that quantification of these gene transcripts is useful for

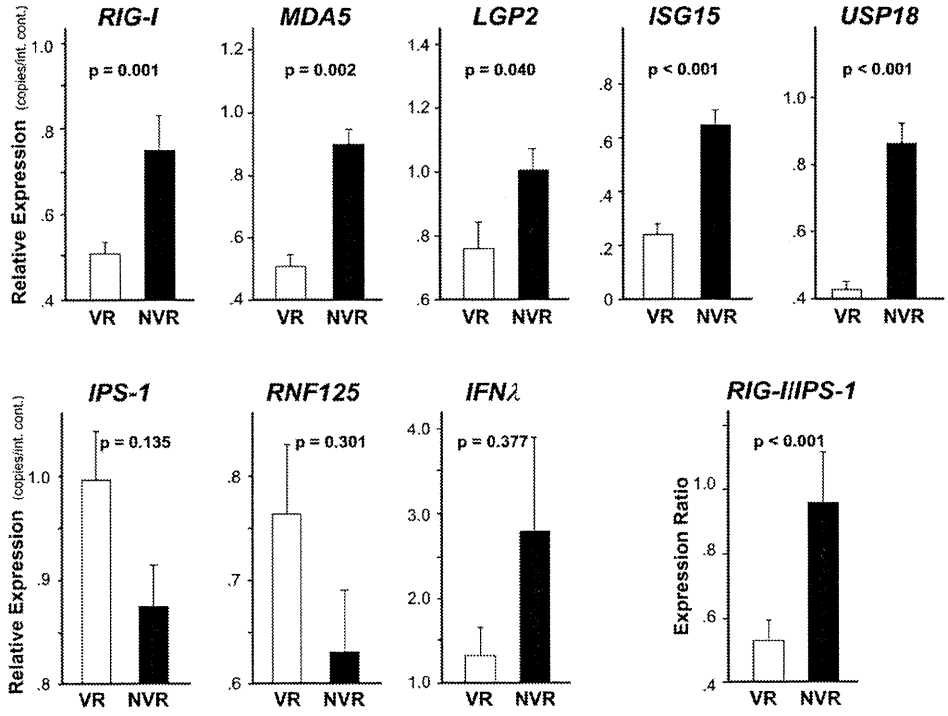

Fig. 2. Comparison of hepatic gene expression levels between virological responders (VR, n = 60) and nonvirological responders (NVR, n = 28). Expression levels of cytoplasmic viral sensors (*RIG-I*, *MDA5*, and *LGP2*), modulators (*ISG15* and *USP18*), an adaptor (*IPS-1*), negative regulators (*RNF125*) and *IFNλ*, and *RIG-I/IPS-1* expression ratio are shown. Error bars indicate standard error. The *P*-values were determined by the Mann-Whitney *U* test.

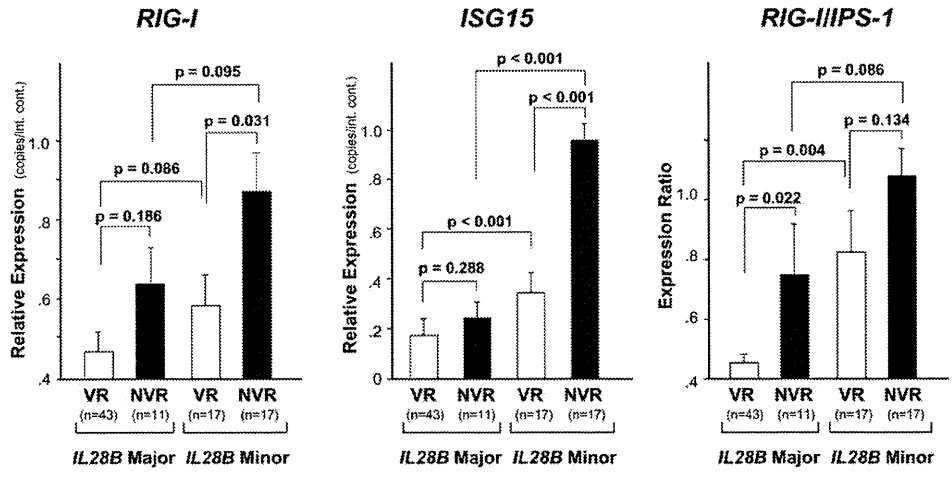

Fig. 3. Comparison of hepatic gene expression levels between virological responders (VR) and nonvirological responders (NVR) in subgroups of the *IL28B* genotype (*IL28B* Major, rs8099917 TT/rs12979860 CC; *IL28B* Minor, rs8099917 TG/rs12979860 CT). Expressions of *RIG-I* and *ISG15* as well as the *RIG-I/IPS-1* expression ratio are shown. Error bars indicate standard error. The numbers of patients in each subgroup are shown in the bottom of the figure.

prediction of NVR (Table 2). The area under the ROC curve for *IL28B* genotype was 0.662, which was lower compared with that for *RIG-I* and *ISG15* expressions and *RIG-I/IPS-1* ratio.

When we stratified the patients by the cutoff value for *RIG-I* and *ISG15* expressions and *RIGI/IPS-1* ratio, no statistically significant difference was found in NVR rates among *IL28B* genotypes within the same subgroup (Fig. 4B).

Factors Associated with NVR. In univariate analysis, age, platelet counts, double mutation at amino acid positions 70 and 91 of the HCV core region, *IL28B* minor allele, and hepatic expressions of *RIG-I, MDA5, LGP2, ISG15*, and *USP18*, and *RIG-I/IPS-1* ratio were significantly

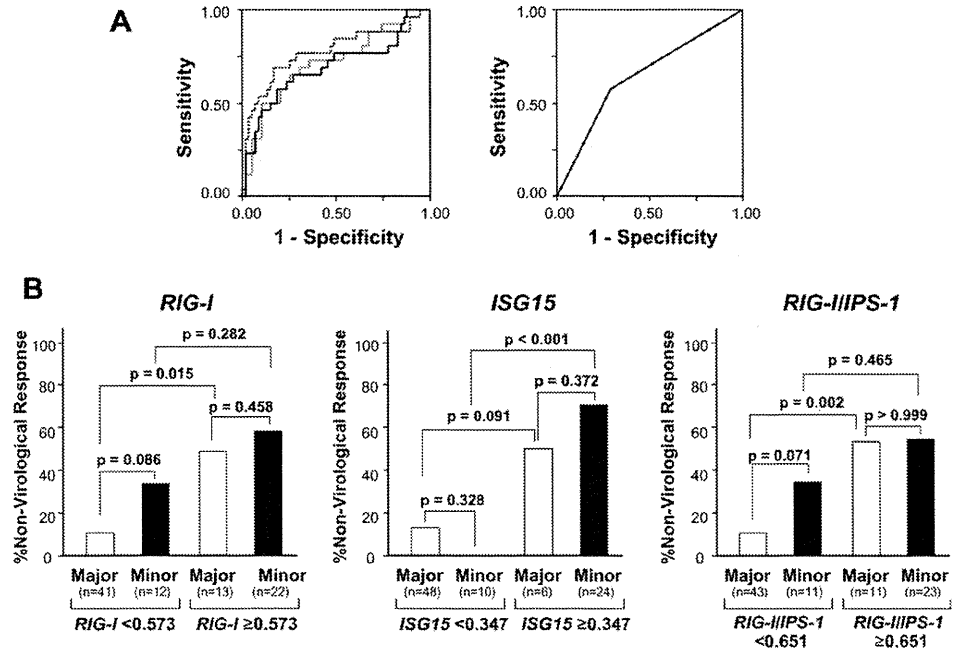

Fig. 4. (A) Receiver operator characteristics (ROC) curve for prediction of nonvirological response. ROC curves were generated to compare *RIG-I* (black line), *ISG15* (dotted line), and *RIG-I/IPS-1* ratio (gray line) (all in the left panel), and *IL28B* genotype (in the right panel). (B) Nonvirological response rate in *IL28B* major (rs8099917 TT/rs12979860 CC) and minor patients (rs8099917 TG/rs12979860 CT) in subgroups divided by the cutoff value of *RIG-I* and *ISG15* expression and the *RIG-I/ISG15* ratio determined by ROC analysis. Cutoff values of *RIG-I* and *ISG15* expression are expressed as expression copy number normalized to the expression of an internal control. The numbers of patients in each subgroup are shown in the bottom of the figure.

Table 2. Area Under the ROC Curves, Sensitivity, Specificity, and Negative as Well as Positive Predictive Values of Nonvirological Responses

Variables	AUC	95% CI	Cutoff	Sensitivity	Specificity	NPV	PPV
RIG-I (copies/int. control)	0.712	0.584-0.840	0.573	0.679	0.733	0.830	0.543
ISG15 (copies/int. control)	0.782	0.666-0.899	0.347	0.714	0.833	0.862	0.667
RIG-I/IPS-1 (copies/int. control)	0.732	0.611-0.852	0.651	0.679	0.750	0.833	0.559
IL28B genotype	0.662	0.537-0.787	TG*/CT†	0.607	0.717	0.796	0.500

AUC, area under the curve; NPV, negative predictive value; PPV, positive predictive value.
*Genotype at rs8099917.
†Genotype at rs12979860.

associated with NVR (Table 3). Among these, multivariate analysis identified old age, HCV core double mutant, and higher hepatic expressions of *RIG-I* and *ISG15* as factors independently associated with NVR (Table 3).

IPS-1 and RIG-I Protein Expression in the Liver. Western blotting revealed that full-length and cleaved IPS-1 were variably present in all the samples from CH-C patients (Fig. 5A). Similar to mRNA

Table 3. Factors Associated with Nonvirological Response

	Univariate Analysis		Multivariate Analysis*	
Factors	Risk Ratio (95% CI)	*P*-value	Risk Ratio (95% CI)	*P*-value
Age (by every 10 year)	1.84 (1.10-3.14)	0.027	3.76 (1.19-11.7)	0.023
Sex				
Male	1			
Female	1.62 (0.59-4.42)	0.350		
BMI (by every 5 kg/m^2)	0.87 (0.46-1.65)	0.672		
Fibrosis stage				
F1/F2	1			
F3/F4	1.82 (0.69-4.85)	0.228		
Degree of steatosis				
<10%	1			
≥10%	1.46 (0.43-5.03)	0.544		
Albumin (by every 1 g/dL)	0.41 (0.11-1.56)	0.190		
AST (by every 40 IU/L)	0.89 (0.53-1.56)	0.681		
ALT (by every 40 IU/L)	0.85 (0.57-1.32)	0.481		
γ-GTP (by every 40 IU/L)	1.32 (0.82-2.07)	0.235		
Fasting blood sugar (by every 100 mg/dL)	1.35 (0.74-2.45)	0.340		
Hemoglobin (by every 1 g/dL)	0.93 (0.67-1.31)	0.683		
Platelet counts (by every 10^4/μL)	0.90 (0.82-0.99)	0.037	0.92 (0.78-1.08)	0.296
HCV load (by every 100 KIU/mL)	1.00 (1.00-1.00)	0.688		
Core 70 & 91 double mutation				
Wild	1		1	
Mutant	3.92 (1.14-13.5)	0.030	11.1 (1.40-88.7)	0.023
ISDR				
Nonwildtype	1			
Wildtype	1.38 (0.13-3.61)	0.513		
IL28B genotype				
Major allele†	1		1	
Minor allele‡	3.91 (1.52-10.0)	0.005	1.53 (0.20-11.9)	0.684
Hepatic gene expression (by every 0.1 copy/*int. control*)				
RIG-I	1.28 (1.10-1.50)	0.002	1.53 (1.07-2.22)	0.021
MDA5	1.53 (1.12-2.00)	0.001		
LGP2	1.34 (1.04-1.74)	0.026		
IPS-1	0.90 (0.78-1.04)	0.143		
RNF125	0.93 (0.83-1.04)	0.204		
ISG15	1.37 (1.16-1.62)	<0.001	1.28 (1.04-1.58)	0.021
USP18	1.67 (1.27-2.20)	<0.001		
IFNλ	1.02 (0.99-1.05)	0.170		
RIG-I/IPS-1 ratio (by every 0.1)	1.21 (1.07-1.36)	0.002		

Risk ratios for nonvirological response were calculated by the logistic regression analysis. BMI, body mass index; AST, aspartate aminotransferase; ALT, alanine aminotransferase; γ-GTP, gamma-glutamyl transpeptidase; HCV, hepatitis C virus; ISDR, IFN sensitivity determining region.
*Multivariate analysis was performed with factors significantly associated with nonvirological response by univariate analysis except for *MDA5*, *LGP2*, *USP18*, and *RIG-I/IPS-1* ratio, which were significantly correlated with *RIG-I* and *ISG15*.
†rs8099917 TT and rs12979860 CC.
‡rs8099917 TG and rs12979860 CT.

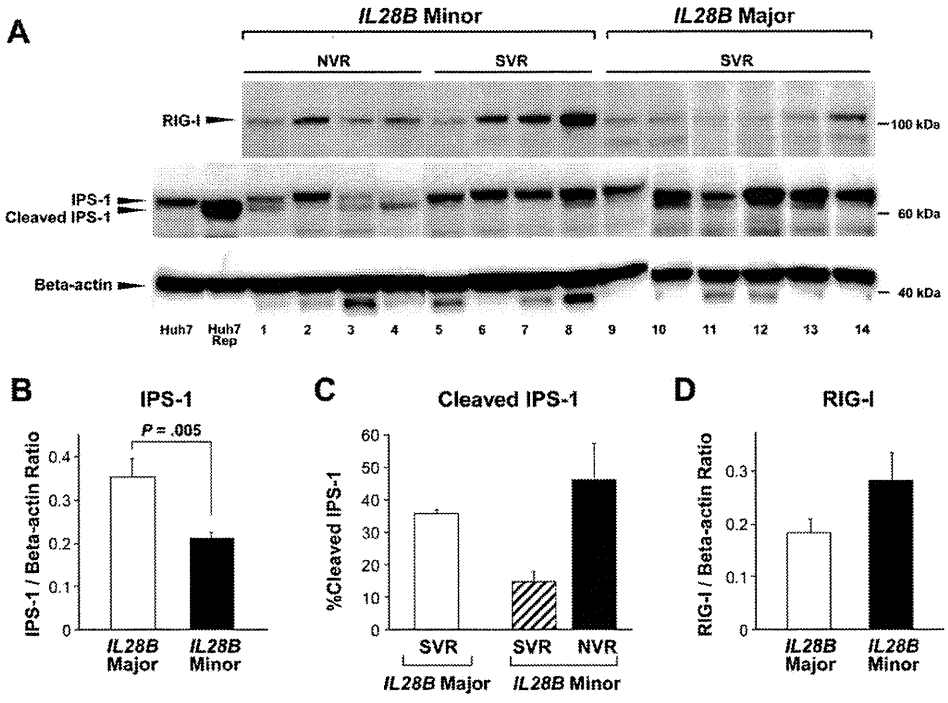

Fig. 5. (A) Western blotting for IPS-1 and RIG-I protein expression levels. Eight lanes contain samples from *IL28B* minor patients (lanes 1-8) and six lanes contain samples from *IL28B* major patients (lanes 9-14). Four lanes contain samples from nonvirological responders (NVR, lanes 1-4) and 10 lanes contain samples from sustained virological responders (SVR, lanes 5-14). Specific bands for RIG-I, full-length IPS-1, cleaved IPS-1, and β-actin are indicated by arrows. Naive Huh7 cells were used for a positive control for full-length IPS-1 (lane Huh7), and cells transfected with HCV-1b subgenomic replicon (Reference #20) were used for a positive control for cleaved IPS-1 (lane Huh7 Rep). (B) Total IPS-1 protein expression levels normalized to β-actin according to *IL28B* genotype. Error bars indicate standard error. *P*-value was determined by Mann-Whitney *U* test. (C) Percentage of cleaved IPS-1 products in total IPS-1 protein according to treatment responses stratified by *IL28B* genotype. Error bars indicate standard error. (D) RIG-I protein expression levels normalized to β-actin according to *IL28B* genotype. Error bars indicate standard error.

expression, total hepatic IPS-1 protein expression was significantly lower in *IL28B* minor patients than in *IL28B* major patients (Fig. 5B). With regard to *IL28B* minor patients, the percentage of cleaved IPS-1 protein in total IPS-1 in SVR was lower than that in NVR (Fig. 5C). In contrast to IPS-1 protein expression, hepatic RIG-I protein expression was higher in *IL28B* minor patients than that in *IL28B* major patients (Fig. 5D).

Discussion

In the present study we found that the baseline expression levels of intrahepatic viral sensors and related regulatory molecules were significantly associated with the genetic variation of *IL28B* and final virological outcome in CH-C patients treated with PEG-IFNα/RBV combination therapy. Although the relationship between the *IL28B* minor allele and NVR in PEG-IFNα/RBV combination therapy is evident, mechanisms responsible for this association remain unknown. *In vitro* studies have suggested that cytoplasmic viral sensors, such as RIG-I and MDA5, play a pivotal role in the regulation of IFN production and augment IFN production through an amplification circuit.[7,8] Our results indicate that expressions of *RIG-I* and *MDA5* and a related amplification system may be up-regulated by endogenous IFN at a higher baseline level in *IL28B* minor patients. However, HCV elimination by subsequent exogenous IFN is insufficient in these patients, as reported,[19] suggesting that *IL28B* minor patients may have adopted a different equilibrium in their innate immune response to HCV. Our data are further supported by recent reports of an association between intrahepatic levels of IFN-stimulated gene expression and PEG-IFNα/RBV response as well as with *IL28B* genotype.[21-23]

In contrast to cytoplasmic viral sensor (*RIG-I, MDA5*, and *LGP2*) and modulator (*ISG15* and *USP18*) expression, the adaptor molecule (*IPS-1*) expression was significantly lower in *IL28B* minor patients. Moreover, western blotting further confirmed IPS-1 protein downregulation in *IL28B* minor patients by revealing decreased protein levels. Because IPS-1 is one of the main target molecules of HCV evasion,[9,18]

transcriptional and translational *IPS-1* expression are probably suppressed by HCV with resistant phenotype, which may be more adaptive in *IL28B* minor patients than in *IL28B* major patients. When we analyzed the proportion of full-length or cleaved IPS-1 to the total IPS-1 protein in a subgroup of *IL28B* minor patients, cleaved IPS-1 product was less dominant in SVR than in NVR, whereas uncleaved full-length IPS-1 protein was more dominant in SVR than in NVR. Therefore, the ability of HCV to evade host innate immunity by cleaving IPS-1 protein and/or host capability of protection from IPS-1 cleavage is probably responsible for the variable treatment responses in *IL28B* minor patients.

Our results indicated a close association between *IL28B* minor patients with higher γ-GTP level and higher frequency of HCV core double mutants, which are known factors for NVR. In contrast, no significant association was observed between *IL28B* genotype and age, gender, or liver fibrosis, which are also known to be unfavorable factors for virological response to PEG-IFNα/RBV. Therefore, certain factors other than the *IL28B* genotype may independently influence virological response. To elucidate whether gene expression involving innate immunity independently associates with a virological response from the *IL28B* genotype, we performed further analysis in a subgroup and conducted a multivariate regression and ROC analyses. Our multivariate and ROC analyses demonstrate that higher expressions of *RIG-I* and *ISG15* as well as a higher ratio of *RIG-I/IPS-1* are independently associated with NVR, and quantification of these values is more useful in predicting final virological response to PEG-IFNα/RBV than determination of *IL28B* genotype in each individual patients. However, the SVR rates in our patients were similar among *IL28B* genotypes, which suggests more SVR patients with the *IL28B* minor allele were included in the present study than those in the general CH-C population. Hence, our data did not necessarily exclude the possibility of the *IL28B* genotype in predicting NVR, although our multivariate analysis could not identify the *IL28B* minor allele as an independent factor for NVR. Interestingly, an association between *IL28B* genotype and expressions of *RIG-I* and *ISG15* as well as *RIG-I/IPS-1* expression ratio is still observed even in patients with the same subgroup of virological response (Fig. 3).

In the present study, although hepatic *IFNλ* expression was observed to be higher in *IL28B* minor and NVR patients, it was not statistically significant. Because *IL28B* shares 98.2% homology with *IL28A*, our primer could not distinguish the expression of *IL28B* from that of *IL28A*, and moreover, we could not specify which cell expresses *IFNλ* (i.e., hepatocytes or other immune cells that have infiltrated the liver). Therefore, the precise mechanisms underlying *IL28B* variation and expression of *IFNλ* in relation to treatment response need further clarification by specifying type of IFNλ and uncovering the producing cells.

In the present study we included genotype 1b patients because it is imperative to designate a virologically homogenous patient group to associate individual treatment responses with different gene expression profiles that direct innate immune responses. We have reported that the *RIG-I/IPS-1* ratio was significantly higher in NVR with HCV genotype 2.[19] However, our preliminary results indicated that baseline hepatic *RIG-I* and *ISG15* expression and the *RIG-I/IPS-1* expression ratio is not significantly different among *IL28B* genotypes in patients infected with genotype 2 (Supporting Figure). This may be related to the rarity of NVR with HCV genotype 2 and the lower effect of *IL28B* genotype on virological responses in patients infected with HCV genotype 2.[24] The association among treatment responses in all genotypes, the different status of innate immune responses, and *IL28B* genotype needs to be examined further.

Differences in allele frequency for *IL28B* SNPs among the population groups has been reported. The frequency of *IL28B* major allele among patients with Asian ancestry is higher than that among patients with European and African ancestry.[25] Because *IL28B* polymorphism strongly influences treatment responses within each population group,[5] our data obtained from Japanese patients can be applied to other population groups. However, the rate of SVR having African ancestry was lower than that having European ancestry within the same *IL28B* genotype.[5] Hence, further study is required to clarify whether this difference among the population groups with the same *IL28B* genotype could be explained by differences in expression of genes involved in innate immunity.

In a recent report, an SVR rate of telaprevir with PEG-IFNα/RBV was only 27.6% in *IL28B* minor patients.[26] Because new anti-HCV therapy should still contain PEG-IFNα/RBV as a platform for the therapy, our findings regarding innate immunity in addressing the mechanism of virological response and predicting NVR remain important in this new era of directly acting anti-HCV agents, such as telaprevir and boceprevir.

In conclusion, this clinical study in humans demonstrates the potential relevance of the molecules involved in innate immunity to the genetic variation

of *IL28B* and clinical response to PEG-IFNα/RBV. Both the *IL28B* minor allele and higher expressions of *RIG-I* and *ISG15* as well as higher *RIG-I/IPS-1* ratio are independently associated with NVR. Innate immune responses in *IL28B* minor patients may have adapted to a different equilibrium compared with that in *IL28B* major patients. Our data will advance both understanding of the pathogenesis of HCV resistance and the development of new antiviral therapy targeted toward the innate immune system.

References

1. Kiyosawa K, Sodeyama T, Tanaka E, Gibo Y, Yoshizawa K, Nakano Y, et al. Interrelationship of blood transfusion, non-A, non-B hepatitis and hepatocellular carcinoma: analysis by detection of antibody to hepatitis C virus. HEPATOLOGY 1990;12:671-675.
2. Zeuzem S, Pawlotsky JM, Lukasiewicz E, von Wagner M, Goulis I, Lurie Y, et al. DITTO-HCV Study Group. International, multicenter, randomized, controlled study comparing dynamically individualized versus standard treatment in patients with chronic hepatitis C. J Hepatol 2005;43:250-257.
3. Tanaka Y, Nishida N, Sugiyama M, Kurosaki M, Matsuura K, Sakamoto N, et al. Genome-wide association of IL28B with response to pegylated IFN-alpha and ribavirin therapy for chronic hepatitis C. Nat Genet 2009;10:1105-1109.
4. Suppiah V, Moldovan M, Ahlenstiel G, Berg T, Weltman M, Abate ML, et al. IL28B is associated with response to chronic hepatitis C IFN-alpha and ribavirin therapy. Nat Genet 2009;10:1100-1104.
5. Ge D, Fellay J, Thompson AJ, Simon JS, Shianna KV, Urban TJ, et al. Genetic variation in IL28B predicts hepatitis C treatment-induced viral clearance. Nature 2009;461:399-401.
6. Biron CA. Initial and innate responses to viral infections—pattern setting in immunity or disease. Curr Opin Microbiol 1999;2:374-381.
7. Yoneyama M, Kikuchi M, Natsukawa T, Shinobu N, Imaizumi T, Miyagishi M, et al. The RNA helicase RIG-I has an essential function in double-stranded RNA-induced innate antiviral responses. Nat Immunol 2004;5:730-737.
8. Yoneyama M, Kikuchi M, Matsumoto K, Imaizumi T, Miyagishi M, Taira K, et al. Shared and unique functions of the DExD/H-box helicases RIG-I, MDA5, and LGP2 in antiviral innate immunity. J Immunol 2005;175:2851-2858.
9. Meylan E, Curran J, Hofmann K, Moradpour D, Binder M, Bartenschlager R, et al. Cardif is an adaptor protein in the RIG-I antiviral pathway and is targeted by hepatitis C virus. Nature 2005;437:1167-1172.
10. Kawai T, Takahashi K, Sato S, Coban C, Kumar H, Kato H, et al. IPS-1, an adaptor triggering RIG-I- and Mda5-mediated type I interferon induction. Nat Immunol 2005;6:981-988.
11. Seth RB, Sun L, Ea CK, Chen ZJ. Identification and characterization of MAVS, a mitochondrial antiviral signaling protein that activates NF-kappaB and IRF 3. Cell 2005;122:669-682.
12. Xu LG, Wang YY, Han KJ, Li LY, Zhai Z, Shu HB. VISA is an adapter protein required for virus-triggered IFN-beta signaling. Mol Cell 2005;19:727-740.
13. Rothenfusser S, Goutagny N, DiPerna G, Gong M, Monks BG, Schoenemeyer A, et al. The RNA helicase Lgp2 inhibits TLR-independent sensing of viral replication by retinoic acid-inducible gene-I. J Immunol 2005;175:5260-5268.
14. Arimoto K, Takahashi H, Hishiki T, Konishi H, Fujita T, Shimotohno K. Negative regulation of the RIG-I signaling by the ubiquitin ligase RNF125. Proc Natl Acad Sci U S A 2007;104:7500-7505.
15. Zhao C, Denison C, Huibregtse JM, Gygi S, Krug RM. Human ISG15 conjugation targets both IFN-induced and constitutively expressed proteins functioning in diverse cellular pathways. Proc Natl Acad Sci U S A 2005;102:10200-10205.
16. Schwer H, Liu LQ, Zhou L, Little MT, Pan Z, Hetherington CJ, et al. Cloning and characterization of a novel human ubiquitin-specific protease, a homologue of murine UBP43 (Usp18). Genomics 2000;65:44-52.
17. Malakhov MP, Malakhova OA, Kim KI, Ritchie KJ, Zhang DE. UBP43 (USP18) specifically removes ISG15 from conjugated proteins. J Biol Chem 2002;277:9976-9981.
18. Li XD, Sun L, Seth RB, Pineda G, Chen ZJ. Hepatitis C virus protease NS3/4A cleaves mitochondrial antiviral signaling protein off the mitochondria to evade innate immunity. Proc Natl Acad Sci U S A 2005;102:17717-17722.
19. Asahina Y, Izumi N, Hirayama I, Tanaka T, Sato M, Yasui Y, et al. Potential relevance of cytoplasmic viral sensors and related regulators involving innate immunity in antiviral response. Gastroenterology 2008;134:1396-1405.
20. Tanabe Y, Sakamoto N, Enomoto N, Kurosaki M, Ueda E, Maekawa S, et al. Synergistic inhibition of intracellular hepatitis C virus replication by combination of ribavirin and interferon-alpha. J Infect Dis 2004;189:1129-1139.
21. Honda M, Sakai A, Yamashita T, Nakamoto Y, Mizukoshi E, Sakai Y, et al. Hepatic ISG expression is associated with genetic variation in interleukin 28B and the outcome of IFN therapy for chronic hepatitis C. Gastroenterology 2010;139:499-509.
22. Urban TJ, Thompson AJ, Bradric SS, Fellay J, Schuppan D, Cronin KD, et al. *IL28B* genotype is associated with differential expression of intrahepatic interferon-stimulated genes in patients with chronic hepatitis C. HEPATOLOGY 2010;52:1888-1896.
23. Dill MT, Duong FHT, Vogt JE, Bibert S, Bochud PY, Terracciano L, et al. Interferon-induced gene expression is a stronger predictor of treatment response than *IL28B* genotype in patients with hepatitis C. Gastroenterology 2011;140:1021-1031.
24. Yu ML, Huang CF, Huang JF, Chang NC, Yang JF, Lin ZY, et al. Role of interleukin-28B polymorphism in the treatment of hepatitis C virus genotype 2 infection in Asian patients. HEPATOLOGY 2011;53:7-13.
25. Thomas DL, Thio CL, Martin MP, Qi Y, Ge D, O'hUigin C, Kidd J, et al. Genetic variation in *IL28B* and spontaneous clearance of hepatitis C virus. Nature 2009;461:798-802.
26. Akuta N, Suzuki F, Hirakawa M, Kawamura Y, Yatsuji H, Sezaki H, et al. Amino acid substitution in hepatitis C virus core region and genetic variation near the interleukin 28B gene predict viral response to teraprevir with pegIFN and ribavirin. HEPATOLOGY 2010;52:421-429.

JOURNAL OF VIROLOGY, June 2011, p. 5986–5994 Vol. 85, No. 12
0022-538X/11/$12.00 doi:10.1128/JVI.02583-10

Analysis of Interferon Signaling by Infectious Hepatitis C Virus Clones with Substitutions of Core Amino Acids 70 and 91▽§

Yusuke Funaoka,[1]† Naoya Sakamoto,[1,2]*† Goki Suda,[1] Yasuhiro Itsui,[1] Mina Nakagawa,[1,2] Sei Kakinuma,[1] Takako Watanabe,[1] Kako Mishima,[1] Mayumi Ueyama,[1] Izumi Onozuka,[1] Sayuri Nitta,[1] Akiko Kitazume,[1] Kei Kiyohashi,[1] Miyako Murakawa,[1] Seishin Azuma,[1] Kiichiro Tsuchiya,[1] and Mamoru Watanabe[1]

Department of Gastroenterology and Hepatology[1] and Department for Hepatitis Control,[2] Tokyo Medical and Dental University, Tokyo, Japan

Received 13 December 2010/Accepted 24 March 2011

Substitution of amino acids 70 and 91 in the hepatitis C virus (HCV) core region is a significant predictor of poor responses to peginterferon-plus-ribavirin therapy, while their molecular mechanisms remain unclear. Here we investigated these differences in the response to alpha interferon (IFN) by using HCV cell culture with R70Q, R70H, and L91M substitutions. IFN treatment of cells transfected or infected with the wild type or the mutant HCV clones showed that the R70Q, R70H, and L91M core mutants were significantly more resistant than the wild type. Among HCV-transfected cells, intracellular HCV RNA levels were significantly higher for the core mutants than for the wild type, while HCV RNA in culture supernatant was significantly lower for these mutants than for the wild type. IFN-induced phosphorylation of STAT1 and STAT2 and expression of the interferon-inducible genes were significantly lower for the core mutants than for the wild type, suggesting cellular unresponsiveness to IFN. The expression level of an interferon signal attenuator, SOCS3, was significantly higher for the R70Q, R70H, and L91M mutants than for the wild type. Interleukin 6 (IL-6), which upregulates SOCS3, was significantly higher for the R70Q, R70H, and L91M mutants than for the wild type, suggesting interferon resistance, possibly through IL-6-induced, SOCS3-mediated suppression of interferon signaling. Expression levels of endoplasmic reticulum (ER) stress proteins were significantly higher in cells transfected with a core mutant than in those transfected with the wild type. In conclusion, HCV R70 and L91 core mutants were resistant to interferon *in vitro*, and the resistance may be induced by IL-6-induced upregulation of SOCS3. Those mechanisms may explain clinical interferon resistance of HCV core mutants.

Hepatitis C virus (HCV) is one of the most important pathogens causing liver-related morbidity and mortality. Approximately 3% of the worldwide population is infected with HCV, which represents 170 million people, and 3 million to 4 million individuals are newly infected each year (33, 47, 62). There is no therapeutic or prophylactic vaccine available for HCV. Antiviral treatment has been shown to improve liver histology and decrease the incidence of hepatocellular carcinoma in chronic hepatitis C (CHC) (17, 64). Current therapies for CHC consist of treatment with pegylated interferon (peg-IFN), which acts both as an antiviral and as an immunoregulatory cytokine, and ribavirin (RBV), an antiviral prodrug that interferes with RNA metabolism (16, 31). However, less than 50% of patients infected with HCV genotype 1 treated in this way achieve a sustained virological response (SVR) or a cure of the infection (14, 16). Given this situations, gaining a detailed understanding of the molecular mechanisms of interferon (IFN) resistance has been a high priority in academia and industry.

The response to peg-IFN-plus-RBV treatment is affected by several viral and host factors, including age, gender (22, 23), grade of liver fibrosis (21, 42), HCV genotype, and serum viral load (14, 59). Several viral genetic factors influence treatment outcomes, including mutations in NS5A-interferon sensitivity determining region (ISDR) (13, 38) and the core region (4, 6). Akuta et al. reported that HCV-core amino acid substitutions at positions 70 and 91 are significantly correlated with poor responses to peg-IFN-plus-RBV therapy (6) and with increased hepatocarcinogenesis (2, 3). Furthermore, it was reported recently that the core amino acid 70 and amino acid 91 substitutions are associated with a poor response to peg-IFN, RBV, and telaprevir combination therapy, respectively (1). However, the underlying molecular mechanisms of such distinct biological properties of the core 70/91 mutations are poorly understood.

In this study, we have analyzed virus infection and replication kinetics and response to interferon treatment using the HCV-JFH1 cell culture system (HCVcc) (60, 65). We constructed HCVcc expressing virus with substitutions of core amino acid 70 and amino acid 91 (R70Q, R70H, and L91M). The core mutant HCV clones were compared in terms of intracellular replication, infectious virus production, and sensitivity to alpha interferon (IFN-α). Here we have shown that the differences in sensitivity to IFN are attributable to upregulated overexpression of the cellular interferon signal attenuator SOCS3 and that this upregulation is caused by overexpression of interleukin-6 (IL-6).

* Corresponding author. Mailing address: Department of Gastroenterology and Hepatology, Tokyo Medical and Dental University, 1-5-45 Yushima, Bunkyo-ku, Tokyo 113-8519, Japan. Phone: 81 3-5803-5877. Fax: 81 3-5803-0268. E-mail: nsakamoto.gast@tmd.ac.jp.
† Y.F. and N.S. contributed equally to this work.
§ Supplemental material for this article may be found at http://jvi.asm.org/.
▽ Published ahead of print on 13 April 2011.

MATERIALS AND METHODS

Reagents. Recombinant human IFN-α2b was from Schering-Plough (Kenilworth, NJ). Beta-mercaptoethanol was from Wako (Osaka, Japan). Antibodies used were SOCS3 and SOCS1, which were from Cell Signaling (Beverly, MA), HCV core (Abcam, Cambridge, MA), NS5A (BioDesign, Saco, ME), GRP78, GADD153/CHOP (Santa Cruz Biotechnology, Santa Cruz, CA), disulfide isomerase (PDI) (Stressgen Biotechnologies, Victoria, British Columbia, Canada), and beta-actin antibody (Sigma). Secondary antibodies were peroxidase-labeled anti-mouse, anti-rabbit antibody (GE Healthcare, Connecticut), donkey anti-goat IgG-horseradish peroxidase (HRP) antibody (Santa Cruz Biotechnology, Santa Cruz, CA), and Alexa 405-labeled goat anti-mouse and Alexa 568-labeled donkey anti-rabbit IgG antibodies (Invitrogen, Carlsbad, CA).

Cells and cell culture. Huh7 cells were maintained in Dulbecco's modified minimal essential medium (DMEM) (Sigma Chemical Co, St. Louis, MO) supplemented with 2 mmol/liter L-glutamine and 10% fetal bovine serum at 37°C under 5.0% CO_2.

Sequence analyses. Nucleotide sequences were read from both strands using BigDye Terminator cycle sequencing ready reaction kits (Applied Biosystems, Foster City, CA) and an automated DNA sequencer (ABI Prism 310 genetic analyzer; Applied Biosystems).

Establishment of mutant HCV clones. In order to introduce various mutations into the core region of JFH1, plasmid pJFH1full was digested with EcoRI and BsiWI, and then the DNA fragment encompassing nucleotides 1 to 456 was subcloned into the pGEM-T Easy vector (Promega, Madison, WI). The following mutations were introduced into the DNA fragment in the subcloning vector by site-directed mutagenesis (Quick-Change II site-directed mutagenesis kit; Stratagene): R70Q, R70H, L91M, and GKPG77-80KKKK. Finally, the EcoRI-BsiWI fragments were subcloned back into the parental plasmid, pJFH1full.

In vitro RNA synthesis and transfection. Full-length HCV expression plasmids were as follows: pJFH1full, which encodes the full-length HCV-JFH1 sequence (60), pR70Q, pR70H, pL91M, and p7780K. These plasmids were linearized at their 3′ ends and used as templates for HCV RNA synthesis using the RiboMax large-scale RNA production system (Promega, Madison, WI). After DNase I (RQ-1 RNase-free DNase; Promega) treatment, the transcribed HCV RNA was purified using Isogen reagent (Nippon Gene, Tokyo, Japan). For the RNA transfection, Huh7 cells were washed twice in phosphate-buffered saline (PBS), and 5×10^6 cells were suspended in Opti-MEM I (Invitrogen, Carlsbad, CA) containing 10 μg of HCV RNA, transferred into a 4-mm electroporation cuvette, and finally subjected to an electric pulse (1,050 μF and 270 V) using the Easy Jet system (EquiBio, Middlesex, United Kingdom). After electroporation, the cell suspension was left for 5 min at room temperature and then incubated under normal culture conditions in a 10-cm-diameter cell culture dish. Forty-eight hours after transfection, the levels of HCV replication and viral protein expression were detected by real-time PCR and Western blotting.

HCVcc infection analyses. Huh7 cells were plated on 12-well plates at a density of 1.2×10^4 cells per well. Supernatants from HCV RNA-transfected cells were inoculated onto each well at a titer of 8×10^5 copies/well (quantified by real-time reverse transcriptase PCR [RT-PCR]). Forty-eight hours after infection, various amounts of interferon were added, and the cells were harvested after 72 h of the interferon treatment (48).

RNA extraction, cDNA synthesis, and real-time RT-PCR analysis. For the detection of HCV RNA in culture supernatant, the supernatant was passed through a 0.45-μm filter (Millex-HA, Millipore, Bedford, MA) and stored at −80°C until use. Protocols and primers for the real-time RT-PCR analysis of HCV RNA have been described previously (48). For the detection of endogenous mRNAs, total cellular RNA was isolated using an RNeasy Mini kit (Qiagen, Valencia, CA). Two micrograms of total cellular RNA was used to generate cDNA from each sample using SuperScript II reverse transcriptase (Invitrogen, Carlsbad, CA). Expression of mRNA was quantified using the TaqMan universal PCR master mix (Applied Biosystems, Foster City, CA) and the ABI 7500 real-time PCR system (Applied Biosystems, Foster City, CA).

Luciferase assays. Luciferase activities were measured using a luminometer (Lumat LB9501; Promega) using the Dual-Luciferase reporter assay system (Promega). Assays were performed in triplicate.

Western blot analysis. Western blotting was carried out as described previously (24, 53, 63). Briefly, 10 mg of total cell lysate was separated using NuPAGE 4%–12% Bis-Tris gels (Invitrogen) and blotted onto a polyvinylidene fluoride (PVDF) Western blotting membrane (Roche). The membrane was incubated with the primary antibodies followed by a peroxidase-labeled anti-IgG antibody and visualized by chemiluminescence using the ECL Western blotting analysis system (Amersham Biosciences, Buckinghamshire, United Kingdom).

Immunohistochemistry. HCV-transfected Huh7 cells were cultured on 18-mm round micro cover glasses (Matsunami, Tokyo, Japan). For detection of HCV core, lipid droplet, and endoplasmic reticulum (ER), cells were fixed with cold acetone for 15 min. The cells were incubated with the primary antibodies for 1 h at 37°C. The fluorescent secondary antibodies were Alexa 405 goat anti-mouse and 568 donkey anti-rabbit IgG antibodies (Invitrogen, Carlsbad, CA). Lipid droplets (LDs) were visualized by using Bodipy 493/503 dye (Invitrogen). Cells were mounted with Vecta Shield mounting medium and 4′,6-diamidino-2-phenylindole (DAPI) (Vector Laboratories, Burlingame, CA) and visualized by using a confocal laser scanning microscope (FV10i; Olympus, Tokyo, Japan).

Calculation of 50% effective concentrations (EC_{50}). The EC_{50} was calculated as the concentration of IFN required for 50% reduction in HCV RNA expression. We used the probit regression analysis to obtain values.

Statistical analyses. Statistical analyses were performed by using Welch's *t* test. *P* values of less than 0.05 were considered statistically significant.

RESULTS

HCV core 70/91 mutants show resistance to IFN treatment. First, we investigated sensitivity to IFN treatment of the HCV core mutant R70Q, R70H, and L91M virus clones and compared them to the wild type. The wild type and core mutants were transfected into Huh7 cells, which were cultured in the presence of various concentrations of IFN-α for 48 h. RNA was extracted from the cells and culture supernatant, and the level of HCV RNA was quantified by real-time RT-PCR. Although the levels of supernatant HCV RNA did not differ between the wild type and core mutants (Fig. 1A), the levels of cellular HCV RNA showed that all three core mutants were significantly resistant to IFN compared to the wild type, with EC_{50}s of 5.0 IU/ml, 48 IU/ml, 32 IU/ml, and 47 IU/ml for the R70Q, R70H, L91M, and mutants and the wild type, respectively (Fig. 1B). To exclude the possible effects on interferon signaling by the input HCV RNA, we performed interferon sensitivity analyses by HCVcc infection. As shown in Fig. 1C, the interferon sensitivities of HCV core mutants and the wild type were consistent with the results of HCV RNA transfection. Similarly, according to Western blotting, the core mutants were more resistant to IFN treatment than the wild type (Fig. 1D).

Core mutants show decreased secretion of viral particles. To determine the mechanisms underlying the resistance to interferon, we compared baseline virus expression levels in cells and culture supernatants. The three core mutants, carrying R70Q, R70H, and L91M, expressed significantly higher levels of intracellular HCV RNA than the wild type, as well as the 7780K clone. (Fig. 2A). 7780K was a negative-control clone that lacked virus particle secretion (37). On the contrary, these core mutants released significantly smaller amounts of HCV RNA into the culture supernatant than the wild type, as well as the negative-control 7780K clone. (Fig. 2B). Consistent with the HCV RNA data, Western blotting showed that cellular HCV core protein levels were higher for the core amino acid 70/91 mutants than the wild type (Fig. 2C). These results suggested that the core 70/91 mutant clones were partially defective in the secretion of infectious virus particles.

Subcellular localization of wild-type and mutant core proteins and lipid droplets. It has been reported that HCV core protein localizes on the cellular LD membrane and may mediate encapsidation of viral genomic RNA and subsequent virus assembly (35, 36). Therefore, we visualized the subcellular localization of wild-type and mutant core proteins in rela-

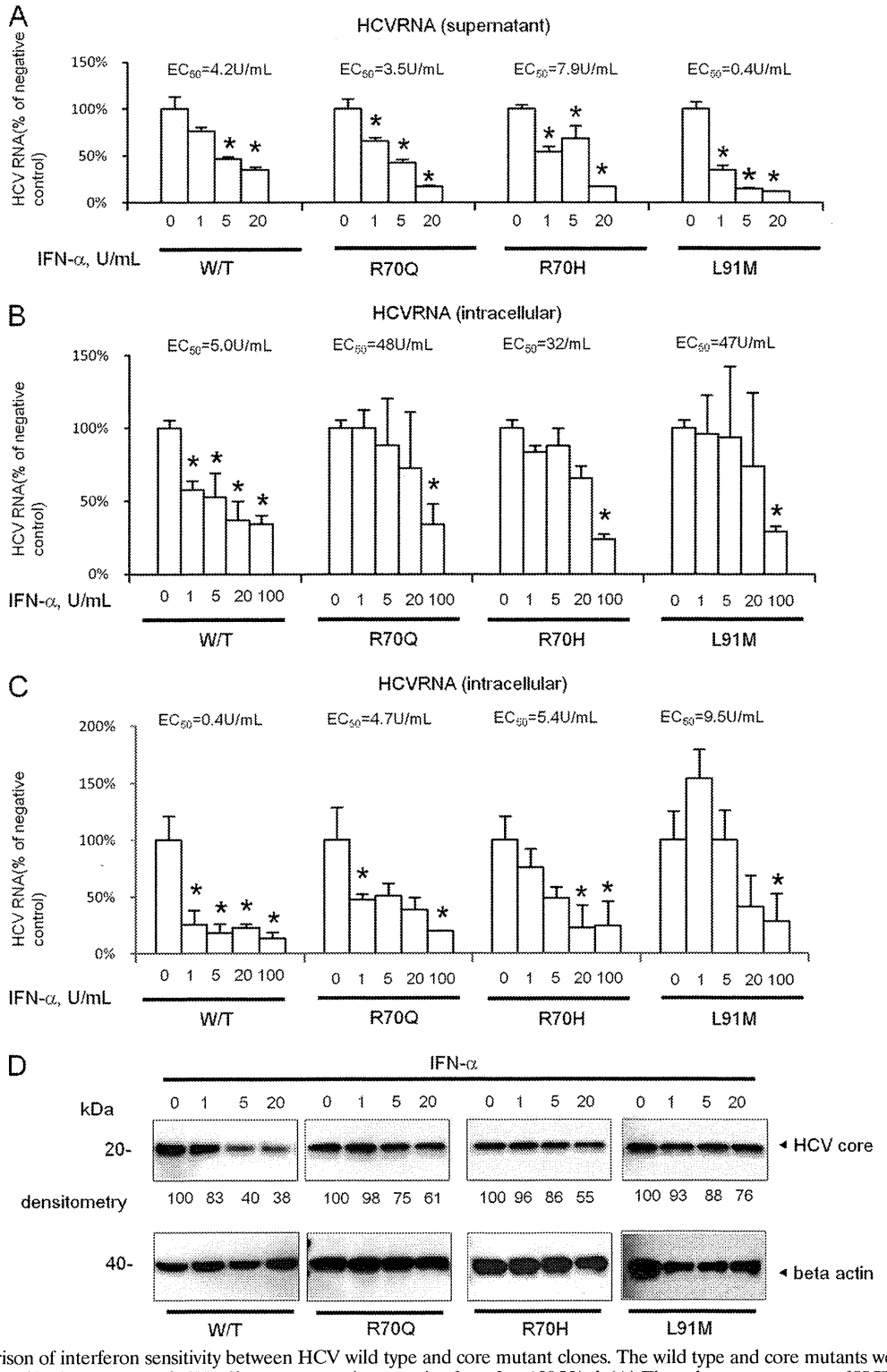

FIG. 1. Comparison of interferon sensitivity between HCV wild type and core mutant clones. The wild type and core mutants were transfected into Huh7 cells and cultured in the presence of IFN-α2b at concentrations ranging from 0 to 100 U/ml. (A) The culture supernatant of HCV-transfected Huh7 cells was collected 72 h after transfection, and the levels of HCV core antigen in the culture supernatant were measured. The values are displayed as percentages of those for the IFN-untreated control. The experiments were repeated three times, and representative results are shown. (B) Expression of intracellular HCV RNA. Cellular RNA was harvested at 72 h posttransfection. HCV RNA was quantified by real-time RT-PCR. The values are displayed as percentages of those for the IFN-untreated control. (C) Expression of intracellular HCV RNA. Cellular RNA was harvested at 72 h postinfection. HCV RNA was quantified by real-time RT-PCR. The values are displayed as percentages of those for the IFN-untreated control. In panels A through C, asterisks indicate *P* values of less than 0.05, compared to results for the interferon-negative control. (D) Western blotting was performed to assess intracellular suppression of HCV core protein. Ten micrograms of harvested cell lysates were subjected to Western blotting using anti-HCV core antibodies. Densitometry of core protein was performed, and results are shown as percentages of the results for an IFN-negative sample.

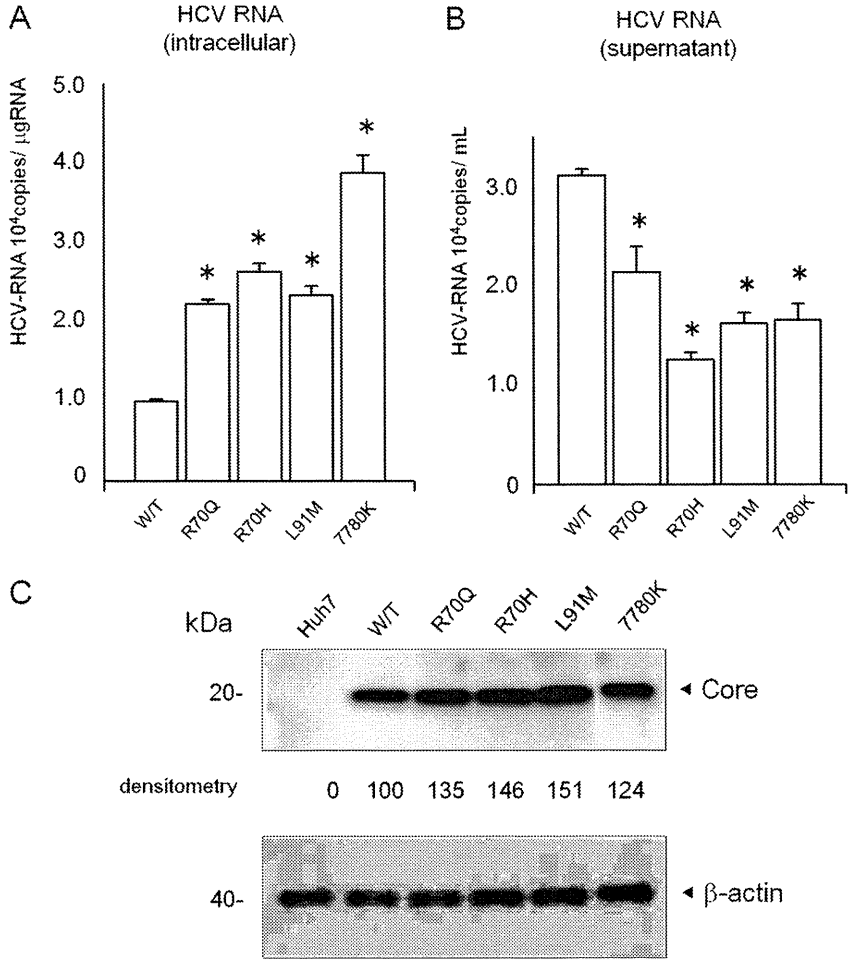

FIG. 2. Analysis of intracellular and supernatant HCV RNA levels in core 70/91 mutants. *In vitro*-transcribed mutant and wild-type RNAs were transfected into Huh7 cells. Three days after transfection, RNA was extracted from cells (A) or culture supernatant (B) and quantified by real-time RT-PCR. Asterisks indicate *P* values of less than 0.05 compared to results for the wild type. (C) Western blotting. Expression of core proteins in HCV-transfected cells. Total cellular protein was prepared from HCV RNA-transfected cells, and Western blotting was performed using anticore and anti-beta-actin antibodies. Densitometry was performed, and results are shown as percentages of that for an HCV-negative sample.

tion to that of LDs and the ER by indirect immunofluorescence and confocal microscopy. Consistent with previous reports, core proteins were colocalized with LDs but not with an ER-located protein, PDI, in the HCV-transfected cells (see the figure in the supplemental material). There were no obvious differences in colocalization of core and LDs or core and ER between the wild type and mutant core proteins.

Induction of interferon-stimulated genes following treatment of HCV-transfected cells with interferon. To investigate the mechanism of the relative IFN resistance of the core 70/91 mutants, as demonstrated in Fig. 1, we analyzed the cellular IFN signaling pathway. First, we assessed the expression and IFN-mediated induction of the mRNA transcripts of the IFN-stimulated genes (ISGs), encoding P56, double-stranded RNA-dependent protein kinase R (PKR), and 2′,5′-oligoadenylate synthetase (25AS), which mediate direct antiviral effects on HCV expression (24, 25). Cellular expression of PKR, P56, and 25AS was substantially increased in HCV-transfected cells, as well as naive cells, following IFN treatment. However, the levels of induction were significantly lower in the three HCV core mutant-transfected cells than in wild-type-transfected cells (Fig. 3A, B, and C). We next detected IFN-induced phosphorylation of STAT1 and STAT2 in the mutant and wild-type HCV-expressing cells. Our previous experiments showed that the levels of phosphorylated STAT1 and STAT2 (pSTAT1 and pSTAT2, respectively) increased within minutes of the addition of IFN and decreased subsequently at 8 h (25). Therefore, we detected pSTAT1 and pSTAT2 levels before and at 15 min after the addition of IFN. As shown in Fig. 3D and E, levels of pSTAT1 and pSTAT2 were lower in core mutant-transfected and -infected cells after IFN treatment than in wild-type-transfected cells and naive cells. These findings indicate that the differences in sensitivity to interferon of core mutant clones and the wild type were associated with attenuation of the cellular IFN signaling pathway.

SOCS3 is upregulated in core mutant clones-transfected, IFN-resistant cells. We examined next the effects of HCV replication on the expression of SOCS1 and SOCS3, proteins that suppress IFN receptor-mediated signaling (50, 58). There was no significant difference in expression levels of SOCS1

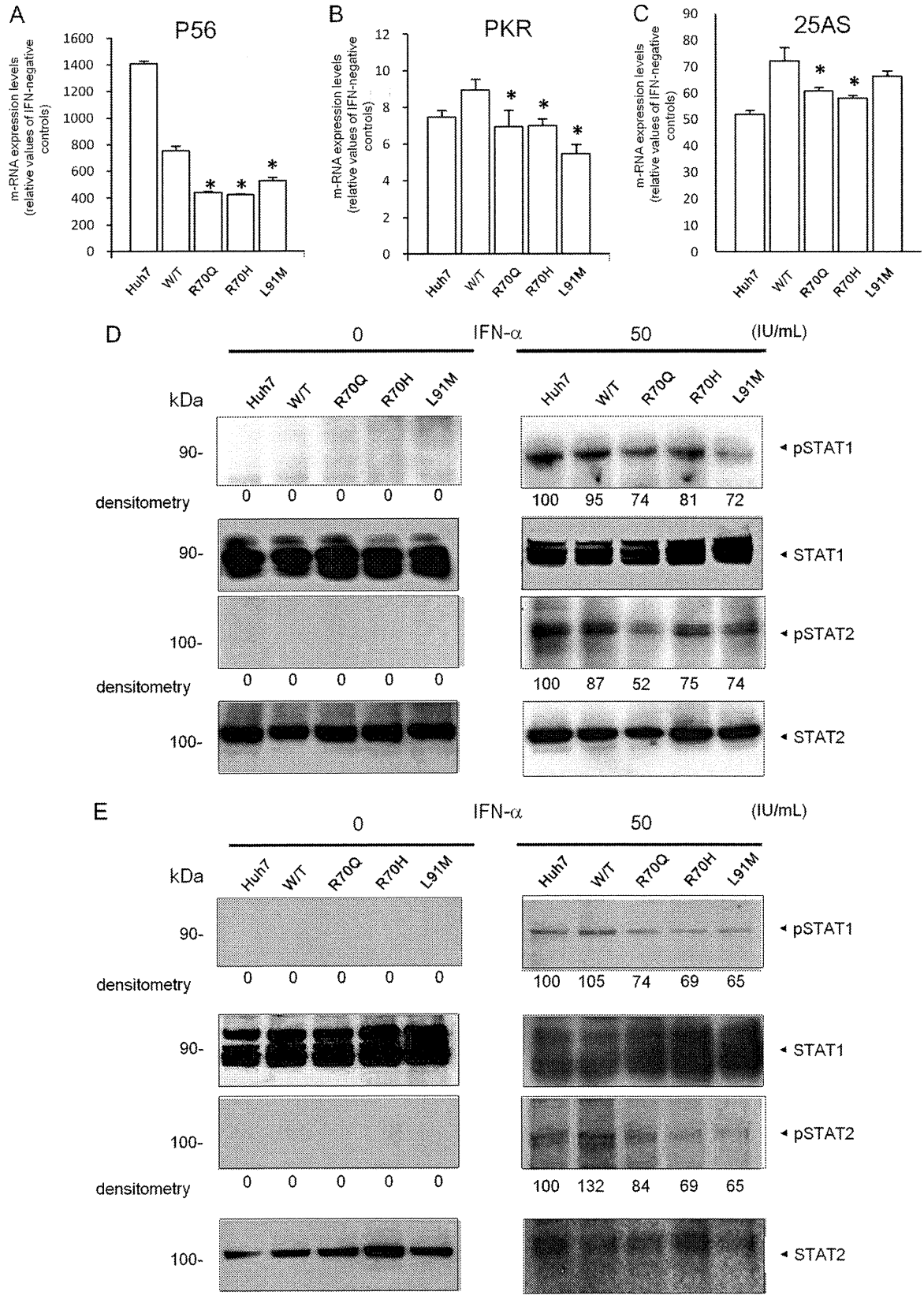

FIG. 3. Interferon-induced expressional induction of the ISGs, P56, PKR, and 25AS in Huh7 cells transfected or infected with wild-type and core mutant JFH1 clones. Two days posttransfection, cells were treated with 50 IU/ml of IFN-α. After 8 h, total cellular RNA was extracted and mRNAs of P56 (A), PKR (B), or 25AS (C) were quantified by real-time RT-PCR analyses. The values are displayed as ratios of IFN-untreated control values. Experiments were repeated three times, and representative results are shown. Asterisks indicate *P* values of less than 0.05 compared to results for the wild type. (D) Western blotting. Expression of total and phosphorylated STAT1 and STAT2 proteins in cells transfected with the wild type and core mutant HCV clones. (E) Western blotting. Expression of total and phosphorylated STAT1 and STAT2 proteins in cells infected with the wild type and core mutant HCV clones. Densitometries for pSTAT1 and pSTAT2 were performed, and results are shown as percentage of results for HCV-negative samples.

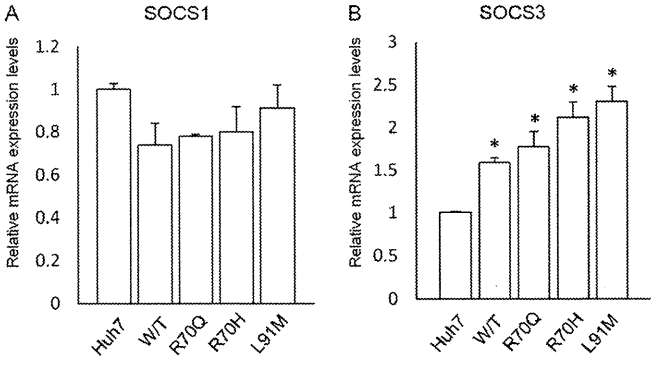

FIG. 4. Effects of core mutant HCV on SOCS1 and SOCS3 expression in Huh7 cells. Expression levels of SOCS1 (A) or SOCS3 (B) in Huh7 cells transfected with the wild type or the core mutant JFH1. Three days posttransfection, total cellular RNA was isolated and the mRNA was quantified by real-time RT-PCR analyses. The experiments were repeated three times, and representative results are shown. The values are displayed as values relative to beta-actin levels. Each experiment was repeated three times, and the representative results are shown. Asterisks indicate P values of less than 0.05 compared to results for the wild type.

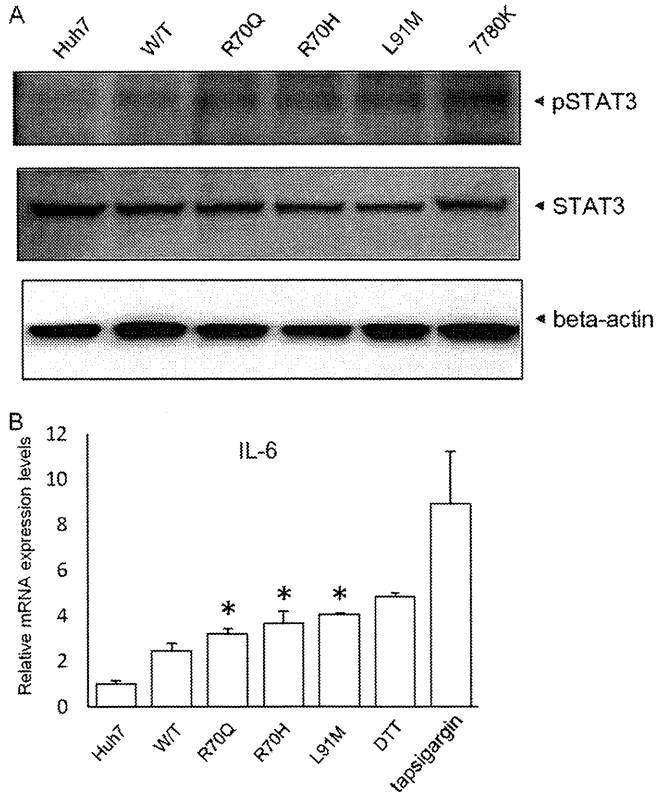

FIG. 5. Expression of phosphorylated STAT3 and IL-6 in cells transfected with the wild type and core mutant HCV-JFH1 clones. (A) Western blotting. Expression of total and phosphorylated STAT3 and beta-actin proteins in cells transfected with the wild type or core mutant HCV clones. (B) Two days posttransfection, total cellular RNA was extracted and mRNAs of IL-6 were quantified by real-time RT-PCR analyses. The values are displayed as the ratio of values of the HCV-untreated control. Asterisks indicate P values of less than 0.05 compared to results for the wild type.

mRNA between cells transfected with the wild type and the core mutant clones. In contrast, the SOCS3 mRNA expression level was significantly higher in core mutant-transfected cells than in wild-type-transfected cells (Fig. 4A and B). It is known that SOCS3 is induced principally by phosphorylated STAT3 (pSTAT3) (18) and that interleukin-6 (IL-6) is a strong inducer of pSTAT3 via receptor-mediated Janus kinase activation in the liver (41, 51). On that basis, we investigated whether overexpression of SOCS3 is associated with increased pSTAT3 and with overproduction of IL-6. The pSTAT3 level was significantly higher in core mutant-transfected cells than in JFH1-transfected cells and naive Huh7 cells (Fig. 5A). Moreover, cellular IL-6 mRNA expression was significantly higher in core mutant-transfected cells than in wild-type-transfected cells (Fig. 5B). These findings suggested that upregulation of cellular SOCS3 is associated with the resistance to IFN of the core 70/91 mutant HCV clones and that this effect is mediated partly by overproduction of IL-6.

UPRs are enhanced in core mutant-transfected cells. We have reported that HCV causes direct cytopathic effects on host cells and that these effects are mediated by HCV-induced unfolded protein responses (UPRs) (48). Therefore, we detected the expression of UPR-related proteins, GRP78 and CHOP, in cells expressing wild-type HCV and the core 70/91 mutants. As shown in Fig. 6, HCV-transfected cells showed higher expression levels of GRP78 and CHOP than untransfected cells. Furthermore, cells transfected with HCV core 70/91 mutant clones expressed larger amounts of GRP78 and CHOP than the wild-type-transfected cells. Because IL-6 is principally expressed following UPR induction (Fig. 5B), these data indicate that HCV-induced UPR may be involved in the IFN resistance of core mutant clones.

DISCUSSION

In this study, we used a virus cell culture system to investigate the characteristics of R70Q, R70H, and L91M HCV core mutant viruses, which were clinically resistant to peg-IFN-plus-RBV treatment, and found that these core mutant clones showed resistance to IFN *in vitro*, consistent with the clinical findings (Fig. 1). These differences in the IFN sensitivity of the core mutant clones led us conduct a series of experiments to investigate the molecular mechanisms of IFN-related response pathways. We found that IFN-α receptor-mediated signaling was attenuated in wild-type HCV-infected and core mutant-infected cells compared to that in uninfected cells and that the suppression of IFN signaling was more potent for core mutant clones than for the wild type. The differences in the interferon-mediated antiviral effects were demonstrated further by the difference in the induction rates of IFN-inducible P56, PKR, and 25AS mRNAs (Fig. 3A, B, and C) and IFN-induced phosphorylation of STAT1 and STAT2 (Fig. 3D and E). Furthermore, the expression levels of an interferon signal attenuator, SOCS3, were significantly higher in core mutant-transfected cells than in wild-type-transfected cells. Moreover, cellular expression of IL-6, which induces SOCS3 expression through phosphorylation of STAT3 (18, 41), was significantly higher in the core mutant-transfected cells than in wild-type-transfected cells (Fig. 5A). Taking all these things together, it is suggested strongly that the IFN resistance of core mutant clones is due to

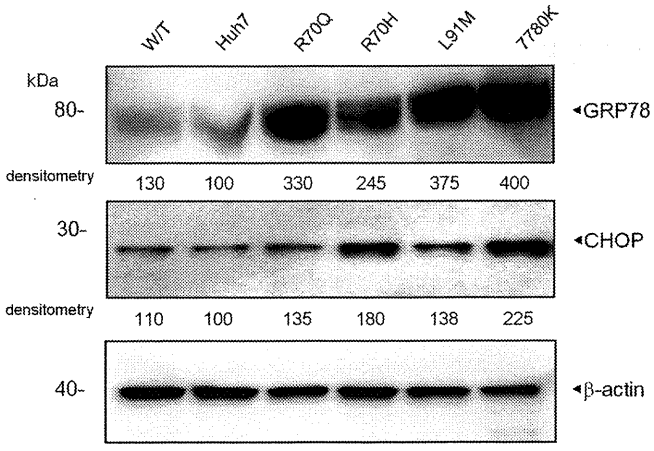

FIG. 6. Expression of GRP78 and CHOP UPR genes in cells transfected with the wild type and core mutant HCV-JFH1 clones. Western blotting was performed to assess UPR following transfection with HCV core mutants. Ten micrograms of harvested cell lysates were subjected to Western blotting using anti-GRP78 and anti-CHOP antibodies. Densitometries for GRP78 and CHOP were performed, and results are shown as percentages of results for uninfected cells.

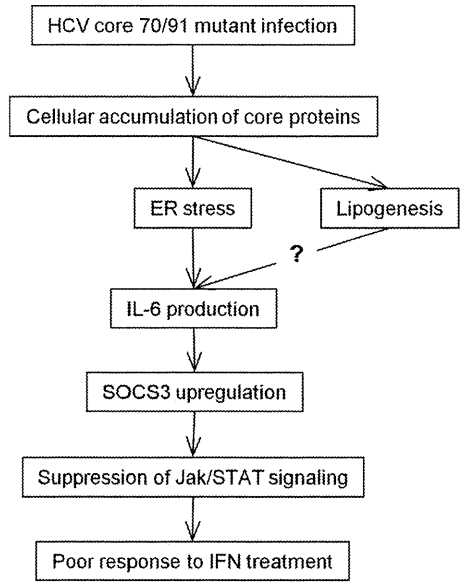

FIG. 7. Schematic diagram of signaling pathway involved in HCV core mutant infection and IFN resistance.

SOCS3-mediated attenuation of IFN responses and that, more importantly, upregulation of cellular IL-6 is attributable to emergence of IFN resistance (Fig. 7).

Miyanari et al. demonstrated that core protein, which is localized in LD-associated membrane, recruits HCV nonstructural (NS) proteins and replication complexes to LD and that this recruitment is critical for producing infectious viruses (35). Furthermore, Masaki et al. reported that the NS5A protein interacts with core at its C-terminal serine cluster and this NS5A-core interaction is crucial for the production of virus particle (32). In this study, there was no difference between the core mutants and the wild-type virus in terms of the pattern of colocalization of core protein with LDs and also the ER membrane (see the figure in the supplemental material). These results suggest that the core amino acid substitutions at positions 70 and 91 do not alter the characteristics of the core protein in terms of subcellular localization. Murray et al. conducted a comprehensive alanine substitution scan of the core protein to search for domains that are essential for virion production. They showed that substitutions of amino acids 70 and 91 spared but slightly decreased the capacity for virus particle production (37), which is consistent with our present results. Those mutations may cause accumulation of virus and core protein in the LDs and ER membrane and may elicit UPRs and IFN resistance.

Type I IFNs and their responsive ISGs are the principal mediators of host defense against virus infections, including HCV (10, 26, 44). Upon binding of IFNs to their receptors, IFNAR1 and IFNAR2, Janus kinases (Jak)1 and 2 phosphorylate STAT1 and STAT2 to form ISGF-3, which translocates to the nucleus and activates transcription of ISGs (46, 54, 55). Members of the SOCS family are potent inhibitors of type I and type III IFN-induced activation of the Jak-STAT pathway and subsequent expression of ISGs (58). HCV, on the other hand, counteracts such IFN-mediated antiviral pathways through its interaction with various steps of IFN signaling. The HCV NS5A and E2 proteins interfere with the action of IFN by inhibiting the activity of PKR (20, 56). NS5A also induces expression of IL-8 and attenuates expression of ISGs (40).

HCV core protein has been reported to interfere with the antiviral actions of IFN. Core protein binds the STAT1-SH domain (29) and destabilizes STAT1 (28) to block IFN signaling. Blindenbacher et al. (8) showed that STAT signaling was strongly inhibited in the hepatocytes of HCV core transgenic mice. Bode et al. showed that HCV core protein induced SOCS3 expression and inhibited tyrosine phosphorylation of STAT1 in HepG2 cells (9). In this study, we used full-length HCV cell culture and found that SOCS3 expression is upregulated at different rates, depending on the genetic sequences of HCV strains, and that these differences in SOCS3 expression are associated with sensitivity to IFN. These results indicate that the IFN resistance of HCV-infected cells is mediated by overexpression of SOCS3, which may be upregulated by HCV proteins, as previously reported (9, 27). Only one amino acid difference, R70Q, R70H, or L91M, might have affected cellular responses to interferon.

IL-6 is the principal activator of STAT3 in hepatocytes (18, 41). It has been reported that plasma IL-6 levels are elevated in CHC patients (30). Basu et al. have conducted DNA microarray analyses in HCV core-expressing cells and demonstrated that genes including those encoding IL-6 and STAT3 were upregulated by core protein (7). Consistent with these findings, we found that cellular IL-6 expression levels were elevated in HCV-transfected cells in the order (from lowest to highest levels) untransfected, wild type, and then core mutants, which correlated well with SOCS3 expression (Fig. 4B) and with cellular responses to IFN (Fig. 1B and C). The inducers of IL-6 remain to be clarified. IL-6 is secreted in response to cellular steatosis and insulin resistance (45). Hepatic steatosis is found in 70% of CHC patients (57) and those with obesity; steatosis or insulin resistance is refractory to IFN treatment (43). Such patients show higher levels of hepatic SOCS3 ex-

pression than those without obesity or insulin resistance (34, 61). We reported previously that a series of genes involved in fatty acid and cholesterol synthesis are upregulated in HCV replicon-expressing and HCV-JFH1-infected cells and increased cellular LDs (39). Such lipogenic cellular processes may be the cause of the upregulated expression of IL-6. Alternatively, UPRs may produce IL-6. Chen et al. have reported that UPRs are coupled with TNF-α and IL-6 production in human macrophages (11). In this study, transfection of Huh7 cells by HCV induced the expression of UPR genes, and their expression levels were significantly higher in mutant core protein-transfected cells than in wild type-transfected cells (Fig. 6).

The differences in ISG expression levels between the HCV wild type and core mutants were significant but small (Fig. 3A, B, and C). As shown in Fig. 3D, and E and 4B, the interclone differences in pSTAT and SOCS3 were significant but relatively small, which may explain the small differences in ISG levels. Similarly, the clinical difference in interferon treatment outcomes between core 70/91 mutants and wild types are significant but are around the sustained viral clearance rates of 32.4% versus 53.5% in core 70 or 91 mutants and wild types, respectively (19), which might be consistent with our present results.

In clinical settings, IFN resistance of the core amino acid 70/91 mutants has been reported for genotype 1b strains (5). At present, there is no report that these mutations are associated with IFN treatment responses to other genotypes, including genotype 2a, which we used in this study. Because HCV strains other than genotypes 1 and 4 are generally sensitive to IFN, the core 70/91 mutations might not affect final treatment outcomes. We have conducted preliminary experiments using genotype 1b infectious clones with low levels of replication and found that these mutations did not significantly affect sensitivity to IFN in culture. It may be necessary to investigate IFN sensitivity when efficient cell culture systems have been developed for HCV genotype 1.

In addition to the poor virological responses of HCV core amino acid 70/91 mutants to peg-IFN-plus-RBV treatment (4, 6, 12), patients infected with the core mutants showed increased incidence of hepatocellular malignancies (2, 15, 49). It has been reported that the HCV core R70 but not L91 mutant frequently causes steatosis and increased hepatic oxidative stress (52). It is possible that core 70/91 mutations not only induce IFN resistance but also may cause other pathophysiological conditions, such as carcinogenesis and disorders of lipid metabolism.

In conclusion, our study demonstrates that the IFN resistance of HCV core mutants may be, for the most part, determined by cellular expression levels of SOCS3 and IL-6. Therapeutic targeting of IL-6 potentially may be a key to targeting IFN resistance and improving antiviral chemotherapeutics against HCV.

ACKNOWLEDGMENTS

We thank Takaji Wakita for providing pJFH1full.

This study was supported by grants from the Ministry of Education, Culture, Sports, Science and Technology—Japan, the Japan Society for the Promotion of Science, Ministry of Health, Labor and Welfare—Japan, Japan Health Sciences Foundation, and National Institute of Biomedical Innovation.

REFERENCES

1. **Akuta, N., et al.** 2010. Amino acid substitution in HCV core region and genetic variation near IL28B gene predict viral response to telaprevir with peginterferon and ribavirin. Hepatology **52:**421–429.
2. **Akuta, N., et al.** 2007. Amino acid substitutions in the hepatitis C virus core region are the important predictor of hepatocarcinogenesis. Hepatology **46:**1357–1364.
3. **Akuta, N., et al.** 2008. Efficacy of low-dose intermittent interferon-alpha monotherapy in patients infected with hepatitis C virus genotype 1b who were predicted or failed to respond to pegylated interferon plus ribavirin combination therapy. J. Med. Virol. **80:**1363–1369.
4. **Akuta, N., et al.** 2007. Predictive factors of early and sustained responses to peginterferon plus ribavirin combination therapy in Japanese patients infected with hepatitis C virus genotype 1b: amino acid substitutions in the core region and low-density lipoprotein cholesterol levels. J. Hepatol. **46:** 403–410.
5. **Akuta, N., et al.** 2005. Virological and biochemical relapse after discontinuation of lamivudine monotherapy for chronic hepatitis B in Japan: comparison with breakthrough hepatitis during long-term treatment. Intervirology **48:**174–182.
6. **Akuta, N., et al.** 2005. Association of amino acid substitution pattern in core protein of hepatitis C virus genotype 1b high viral load and non-virological response to interferon-ribavirin combination therapy. Intervirology **48:**372–380.
7. **Basu, A., et al.** 2006. Microarray analyses and molecular profiling of Stat3 signaling pathway induced by hepatitis C virus core protein in human hepatocytes. Virology **349:**347–358.
8. **Blindenbacher, A., et al.** 2003. Expression of hepatitis c virus proteins inhibits interferon alpha signaling in the liver of transgenic mice. Gastroenterology **124:**1465–1475.
9. **Bode, J. G., et al.** 2003. IFN-alpha antagonistic activity of HCV core protein involves induction of suppressor of cytokine signaling-3. FASEB J. **17:**488–490.
10. **Chang, K. C., E. Hansen, L. Foroni, J. Lida, and G. Goldspink.** 1991. Molecular and functional analysis of the virus- and interferon-inducible human MxA promoter. Arch. Virol. **117:**1–15.
11. **Chen, L., et al.** 2009. HIV protease inhibitor lopinavir-induced TNF-alpha and IL-6 expression is coupled to the unfolded protein response and ERK signaling pathways in macrophages. Biochem. Pharmacol. **78:**70–77.
12. **Donlin, M. J., et al.** 2007. Pretreatment sequence diversity differences in the full-length hepatitis C virus open reading frame correlate with early response to therapy. J. Virol. **81:**8211–8224.
13. **Enomoto, N., et al.** 1996. Mutations in the nonstructural protein 5A gene and response to interferon in patients with chronic hepatitis C virus 1b infection. N. Engl. J. Med. **334:**77–81.
14. **Farci, P., et al.** 2002. Early changes in hepatitis C viral quasispecies during interferon therapy predict the therapeutic outcome. Proc. Natl. Acad. Sci. U. S. A. **99:**3081–3086.
15. **Fishman, S. L., et al.** 2009. Mutations in the hepatitis C virus core gene are associated with advanced liver disease and hepatocellular carcinoma. Clin. Cancer Res. **15:**3205–3213.
16. **Fried, M. W., et al.** 2002. Peginterferon alfa-2a plus ribavirin for chronic hepatitis C virus infection. N. Engl. J. Med. **347:**975–982.
17. **George, S. L., et al.** 2009. Clinical, virologic, histologic, and biochemical outcomes after successful HCV therapy: a 5-year follow-up of 150 patients. Hepatology **49:**729–738.
18. **Hanada, T., I. Kinjyo, K. Inagaki-Ohara, and A. Yoshimura.** 2003. Negative regulation of cytokine signaling by CIS/SOCS family proteins and their roles in inflammatory diseases. Rev. Physiol. Biochem. Pharmacol. **149:**72–86.
19. **Hayes, C. N., et al.** 2010. HCV substitutions and IL28B polymorphisms on outcome of peg-interferon plus ribavirin combination therapy. Gut **60:**261–267.
20. **He, Y., and M. G. Katze.** 2002. To interfere and to anti-interfere: the interplay between hepatitis C virus and interferon. Viral Immunol. **15:**95–119.
21. **Heathcote, E. J., et al.** 2000. Peginterferon alfa-2a in patients with chronic hepatitis C and cirrhosis. N. Engl. J. Med. **343:**1673–1680.
22. **Honda, T., et al.** 2007. Efficacy of ribavirin plus interferon-alpha in patients aged >or=60 years with chronic hepatitis C. J. Gastroenterol. Hepatol. **22:**989–995.
23. **Hung, C. H., et al.** 2008. Association of amino acid variations in the NS5A and E2-PePHD region of hepatitis C virus 1b with hepatocellular carcinoma. J. Viral Hepat. **15:**58–65.
24. **Itsui, Y., et al.** 2009. Antiviral effects of the interferon-induced protein guanylate binding protein 1 and its interaction with the hepatitis C virus NS5B protein. Hepatology **50:**1727–1737.
25. **Itsui, Y., et al.** 2006. Expressional screening of interferon-stimulated genes for antiviral activity against hepatitis C virus replication. J. Viral Hepat. **13:**690–700.
26. **Kalvakolanu, D. V.** 2003. Alternate interferon signaling pathways. Pharmacol. Ther. **100:**1–29.

27. **Kawaguchi, T., et al.** 2004. Hepatitis C virus down-regulates insulin receptor substrates 1 and 2 through up-regulation of suppressor of cytokine signaling 3. Am. J. Pathol. **165:**1499–1508.
28. **Lin, W., et al.** 2005. Hepatitis C virus expression suppresses interferon signaling by degrading STAT1. Gastroenterology **128:**1034–1041.
29. **Lin, W., et al.** 2006. Hepatitis C virus core protein blocks interferon signaling by interaction with the STAT1 SH2 domain. J. Virol. **80:**9226–9235.
30. **Malaguarnera, M., et al.** 1997. Elevation of interleukin 6 levels in patients with chronic hepatitis due to hepatitis C virus. J. Gastroenterol. **32:**211–215.
31. **Manns, M. P., et al.** 2001. Peginterferon alfa-2b plus ribavirin compared with interferon alfa-2b plus ribavirin for initial treatment of chronic hepatitis C: a randomised trial. Lancet **358:**958–965.
32. **Masaki, T., et al.** 2008. Interaction of hepatitis C virus nonstructural protein 5A with core protein is critical for the production of infectious virus particles. J. Virol. **82:**7964–7976.
33. **Massard, J., et al.** 2006. Natural history and predictors of disease severity in chronic hepatitis C. J. Hepatol. **44:**S19–S24.
34. **Miyaaki, H., et al.** 2009. Predictive value of suppressor of cytokine signal 3 (SOCS3) in the outcome of interferon therapy in chronic hepatitis C. Hepatol. Res. **39:**850–855.
35. **Miyanari, Y., et al.** 2007. The lipid droplet is an important organelle for hepatitis C virus production. Nat. Cell Biol. **9:**1089–1097.
36. **Moradpour, D., C. Englert, T. Wakita, and J. R. Wands.** 1996. Characterization of cell lines allowing tightly regulated expression of hepatitis C virus core protein. Virology **222:**51–63.
37. **Murray, C. L., C. T. Jones, J. Tassello, and C. M. Rice.** 2007. Alanine scanning of the hepatitis C virus core protein reveals numerous residues essential for production of infectious virus. J. Virol. **81:**10220–10231.
38. **Nakagawa, M., et al.** 2010. Mutations in the interferon sensitivity determining region and virological response to combination therapy with pegylated-interferon alpha 2b plus ribavirin in patients with chronic hepatitis C-1b infection. J. Gastroenterol. **45:**656–665.
39. **Nishimura-Sakurai, Y., et al.** 2010. Comparison of HCV-associated gene expression and cell signaling pathways in cells with or without HCV replicon and in replicon-cured cells. J. Gastroenterol. **45:**523–536.
40. **Polyak, S. J., K. S. Khabar, M. Rezeiq, and D. R. Gretch.** 2001. Elevated levels of interleukin-8 in serum are associated with hepatitis C virus infection and resistance to interferon therapy. J. Virol. **75:**6209–6211.
41. **Ramadori, G., and B. Christ.** 1999. Cytokines and the hepatic acute-phase response. Semin. Liver Dis. **19:**141–155.
42. **Roffi, L., et al.** 2008. Pegylated interferon-alpha2b plus ribavirin: an efficacious and well-tolerated treatment regimen for patients with hepatitis C virus related histologically proven cirrhosis. Antivir. Ther. **13:**663–673.
43. **Romero-Gomez, M., et al.** 2005. Insulin resistance impairs sustained response rate to peginterferon plus ribavirin in chronic hepatitis C patients. Gastroenterology **128:**636–641.
44. **Ronni, T., et al.** 1998. The proximal interferon-stimulated response elements are essential for interferon responsiveness: a promoter analysis of the antiviral MxA gene. J. Interferon Cytokine Res. **18:**773–781.
45. **Sabio, G., et al.** 2008. A stress signaling pathway in adipose tissue regulates hepatic insulin resistance. Science **322:**1539–1543.
46. **Samuel, C.** 2001. Antiviral actions of interferons. Clin. Microbiol. Rev. **14:**778–809.
47. **Santantonio, T., et al.** 2003. Natural course of acute hepatitis C: a long-term prospective study. Dig. Liver Dis. **35:**104–113.
48. **Sekine-Osajima, Y., et al.** 2008. Development of plaque assays for hepatitis C virus-JFH1 strain and isolation of mutants with enhanced cytopathogenicity and replication capacity. Virology **371:**71–85.
49. **Sobesky, R., et al.** 2007. Distinct hepatitis C virus core and F protein quasispecies in tumoral and nontumoral hepatocytes isolated via microdissection. Hepatology **46:**1704–1712.
50. **Song, M. M., and K. Shuai.** 1998. The suppressor of cytokine signaling (SOCS) 1 and SOCS3 but not SOCS2 proteins inhibit interferon-mediated antiviral and antiproliferative activities. J. Biol. Chem. **273:**35056–35062.
51. **Suda, G., et al.** 2010. IL-6-mediated intersubgenotypic variation of interferon sensitivity in hepatitis C virus genotype 2a/2b chimeric clones. Virology **407:**80–90.
52. **Tachi, Y., et al.** 2010. Impact of amino acid substitutions in the hepatitis C virus genotype 1b core region on liver steatosis and hepatic oxidative stress in patients with chronic hepatitis C. Liver Int. **30:**554–559.
53. **Tanabe, Y., et al.** 2004. Synergistic inhibition of intracellular hepatitis C virus replication by combination of ribavirin and interferon-alpha. J. Infect. Dis. **189:**1129–1139.
54. **Taniguchi, T., K. Ogasawara, A. Takaoka, and N. Tanaka.** 2001. IRF family of transcription factors as regulators of host defense. Annu. Rev. Immunol. **19:**623–655.
55. **Taniguchi, T., and A. Takaoka.** 2002. The interferon-alpha/beta system in antiviral responses: a multimodal machinery of gene regulation by the IRF family of transcription factors. Curr. Opin. Immunol. **14:**111–116.
56. **Taylor, D. R., S. T. Shi, P. R. Romano, G. N. Barber, and M. M. Lai.** 1999. Inhibition of the interferon-inducible protein kinase PKR by HCV E2 protein. Science **285:**107–110.
57. **Vidali, M., et al.** 2008. Interplay between oxidative stress and hepatic steatosis in the progression of chronic hepatitis C. J. Hepatol. **48:**399–406.
58. **Vlotides, G., et al.** 2004. SOCS-1 and SOCS-3 inhibit IFN-alpha-induced expression of the antiviral proteins 2,5-OAS and MxA. Biochem. Biophys. Res. Commun. **320:**1007–1014.
59. **von Wagner, M., et al.** 2003. Dynamics of hepatitis C virus quasispecies turnover during interferon-alpha treatment. J. Viral Hepat. **10:**413–422.
60. **Wakita, T., et al.** 2005. Production of infectious hepatitis C virus in tissue culture from a cloned viral genome. Nat. Med. **11:**791–796.
61. **Walsh, M. J., et al.** 2006. Non-response to antiviral therapy is associated with obesity and increased hepatic expression of suppressor of cytokine signalling 3 (SOCS-3) in patients with chronic hepatitis C, viral genotype 1. Gut **55:**529–535.
62. **Wiese, M., et al.** 2005. Outcome in a hepatitis C (genotype 1b) single source outbreak in Germany—a 25-year multicenter study. J. Hepatol. **43:**590–598.
63. **Yokota, T., et al.** 2003. Inhibition of intracellular hepatitis C virus replication by synthetic and vector-derived small interfering RNAs. EMBO Rep. **4:**602–608.
64. **Yoshida, H., et al.** 2004. Benefit of interferon therapy in hepatocellular carcinoma prevention for individual patients with chronic hepatitis C. Gut **53:**425–430.
65. **Zhong, J., et al.** 2005. Robust hepatitis C virus infection in vitro. Proc. Natl. Acad. Sci. U. S. A. **102:**9294–9299.

ANTIMICROBIAL AGENTS AND CHEMOTHERAPY, June 2011, p. 2537–2545 Vol. 55, No. 6
0066-4804/11/$12.00 doi:10.1128/AAC.01780-10

Inhibitory Effect of a Triterpenoid Compound, with or without Alpha Interferon, on Hepatitis C Virus Infection▽†

Takako Watanabe,[1]‡ Naoya Sakamoto,[1,2]‡* Mina Nakagawa,[1,2] Sei Kakinuma,[1,2] Yasuhiro Itsui,[3] Yuki Nishimura-Sakurai,[1] Mayumi Ueyama,[1] Yusuke Funaoka,[1] Akiko Kitazume,[1] Sayuri Nitta,[1] Kei Kiyohashi,[1] Miyako Murakawa,[1] Seishin Azuma,[1] Kiichiro Tsuchiya,[1] Shinya Oooka,[1] and Mamoru Watanabe[1]

Department of Gastroenterology and Hepatology[1] and Department for Hepatitis Control,[2] Tokyo Medical and Dental University, Tokyo, Japan, and Department of Internal Medicine, Soka Municipal Hospital, Saitama, Japan[3]

Received 19 December 2010/Returned for modification 11 January 2011/Accepted 14 March 2011

A lack of patient response to alpha interferon (α-IFN) plus ribavirin (RBV) treatment is a major problem in eliminating hepatitis C virus (HCV). We screened chemical libraries for compounds that enhanced cellular responses to α-IFN and identified a triterpenoid, toosendanin (TSN). Here, we studied the effects and mechanisms of action of TSN on HCV replication and its effect on α-IFN signaling. We treated HCV genotype 1b replicon-expressing cells and HCV-J6/JFH-infected cells with TSN, with or without α-IFN, and the level of HCV replication was quantified. To study the effects of TSN on α-IFN signaling, we detected components of the interferon-stimulated gene factor 3 (ISGF3), phosphorylated signal transducer and activator of transcription 1 (STAT1), and STAT2 by Western blotting analysis; expression levels of mRNA of interferon regulatory factor 9 using real-time reverse transcription-PCR (RT-PCR); and interferon-stimulated response element reporter activity and measured the expression levels of interferon-inducible genes for 2′,5′-oligoadenylate synthetase, MxA, protein kinase R, and p56 using real-time RT-PCR. TSN alone specifically inhibited expression of the HCV replicon (50% effective concentration = 20.6 nM, 50% cytotoxic concentration > 3 μM, selectivity index > 146). Pretreatment with TSN prior to α-IFN treatment was more effective in suppressing HCV replication than treatment with either drug alone. Although TSN alone did not activate the α-IFN pathway, it significantly enhanced the α-IFN-induced increase of phosphorylated STATs, interferon-stimulated response element activation, and interferon-stimulated gene expression. TSN significantly increased baseline expression of interferon regulatory factor 9, a component of interferon-stimulated gene factor 3. Antiviral effects of treatment with α-IFN can be enhanced by pretreatment with TSN. Its mechanisms of action could potentially be important to identify novel molecular targets to treat HCV infection.

Hepatitis C virus (HCV) is one of the most important pathogens causing acute and chronic hepatitis, liver cirrhosis, and hepatocellular malignancies (29). Alpha interferon (α-IFN) combined with ribavirin (RBV) is the standard treatment for HCV infection (6, 10). However, virus elimination rates are about 50% among treated patients, and therapy is often accompanied by substantial side effects (6, 44). It was recently reported that genetic polymorphisms of the *IL28B* gene, which codes for lambda IFN, are critical for predicting responses to α-IFN plus RBV therapy (8, 35, 38). Patients with minor variants of *IL28B*, who comprise ~50% of Caucasian, 25% of Asian, and ~70% of African populations, showed poor responses to α-IFN treatment. Although new specific anti-HCV drugs are under development, many of them require combined use with α-IFN and RBV (26). Taken together, current difficulties in eliminating HCV are mostly attributable to the limited treatment options and to the limited activity of α-IFN against the virus. For this reason, the development of safe and effective agents that enhance antiviral actions against HCV has been a strong motivation in academia and industry.

To search for a new agent which enhances the effect of α-IFN, we used interferon-stimulated response element (ISRE) reporter screening. We screened a chemical library (60,500 compounds) for compounds that enhance ISRE activity when they are used in combination with α-IFN, using ISRE reporter screening, and identified several compounds that increased the ISRE reporter activities when they are used in combination with α-IFN and that did not show cytotoxicity. Among the hit compounds, toosendanin (TSN; $C_{30}H_{38}O_{11}$; molecular weight = 574) (Fig. 1), which is a triterpenoid derivative extracted from the bark of *Melia toosendan* Sieb et Zucc, was the strongest in enhancing α-IFN-induced ISRE reporter activation and the expression of interferon-stimulated genes (ISGs). TSN has been used as an anthelmintic vermifuge against ascaris (31). Although TSN has some other biological effects against toxin-producing anaerobic bacteria and against carcinoma cells (32, 45), antiviral activity has not been reported.

In this study, we showed, using an HCV replicon system, that TSN, with or without α-IFN, inhibits HCV replication in a cultured human hepatoma Huh7 cell line and that the combination of TSN and α-IFN shows synergistic effects on viral replication. We have investigated the mechanisms of action of

* Corresponding author. Mailing address: Department of Gastroenterology and Hepatology, Tokyo Medical and Dental University, 1-5-45 Yushima, Bunkyo-ku, Tokyo 113-8519, Japan. Phone: 81 3-5803-5877. Fax: 81 3-5803-0268. E-mail: nsakamoto.gast@tmd.ac.jp.

† Supplemental material for this article may be found at http://aac.asm.org/.

‡ T.W. and N.S. contributed equally to this work.

▽ Published ahead of print on 28 March 2011.

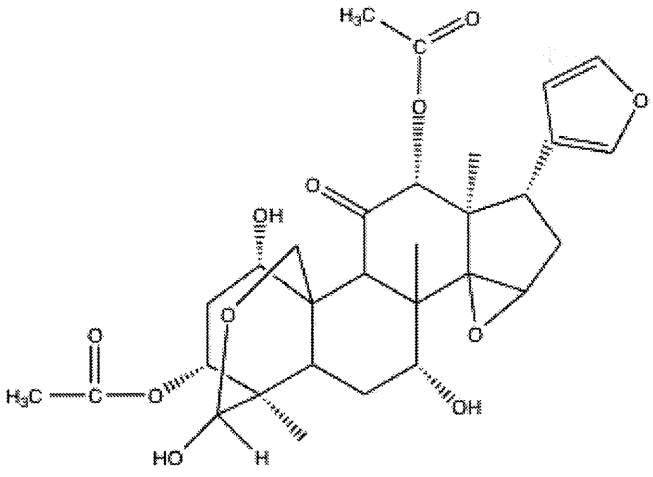

FIG. 1. Chemical structure of toosendanin.

TSN further and show that TSN induced activation of a component of interferon-stimulated gene factor 3 (ISGF3).

MATERIALS AND METHODS

Reagents. Alpha interferon was from Otsuka (Tokushima, Japan). TSN was from APIN Chemicals (Oxon, United Kingdom). Purity was over 77.32%. The designated concentration was achieved through dilution with cell culture medium (the final concentration of dimethyl sulfoxide [DMSO] in the medium was less than 0.3%). Beta-mercaptoethanol was from Wako (Osaka, Japan). The TSN used in this study was solubilized in DMSO.

Cells and cell culture. The human hepatoma cell line Huh7 was maintained in Dulbecco's modified Eagle's medium (Sigma, St. Louis, MO) supplemented with 10% fetal bovine serum at 37°C under 5% CO_2. To maintain cell lines carrying an HCV subgenomic replicon (Huh7/Rep-Feo), G418 (Nakalai Tesque, Kyoto, Japan) was added to the culture medium at a final concentration of 500 μg/ml.

HCV subgenomic replicon construct. The HCV subgenomic replicon plasmid pRep-Feo expresses a fusion gene comprising the firefly luciferase and neomycin phosphotransferase (37, 43). RNA was synthesized *in vitro* from the plasmid and transfected into Huh7 cells. After culture in the presence of G418, cell lines stably expressing the replicon were established.

Reporter constructs. We analyzed the effects of TSN, with or without α-IFN, on signal transduction of ISRE and nuclear factor-kappaB (NF-kappaB). A plasmid, pCIneo-Rluc-IRES-Fluc, was constructed to analyze HCV internal ribosome entry site (IRES)-mediated translation efficiency (23). Plasmids pISRE-TA-Luc and pNF-kappaB-Luc (Clontech Laboratories, Franklin Lakes, NJ) contained consensus motifs upstream of the firefly luciferase gene. A plasmid, pTA-Luc (Clontech), which lacks the enhancer element, was used to determine the background. Plasmid pRL-CMV (Promega, Madison, WI), which expresses the Renilla luciferase protein, was used for normalization of transfection efficiency (17).

ISRE reporter screening. Huh7 cells were seeded in 384-well plates at a density of 3.0×10^3 cells/well. An ISRE-responsive firefly luciferase reporter was introduced using Lipofectamine 2000 (Invitrogen). Five hours after transfection, the cells were treated with 60,500 compounds from chemical libraries at a concentration of 3 μg/ml for 24 h and then treated with α-IFN at a concentration of 3 IU/ml. Six hours later, cells were lysed, and luciferase activities were quantified using a Steady Glo luciferase assay kit (Promega). The compounds were stored in 100% DMSO, and thus, the final concentration of DMSO was 0.3%. *Z'* factors were calculated as reported previously (46).

Luciferase assays and measurements of antiviral activity. Huh7/Rep-Feo cells were cultured with various concentrations of compound, such that the final DMSO concentration was 0.1%. Levels of HCV replication were quantified by internal luciferase assay after 48 h of culture. Luciferase activities were quantified using a luminometer (Promega) and the Bright-Glo luciferase assay system (Promega). Assays were performed in triplicate, and the results are expressed as mean percentage of the controls ± standard deviation (SD). The 50% effective concentration (EC_{50}) values were calculated using the probit method (2, 33). The determination of EC_{50}s was performed three times, and EC_{50}s are presented as means ± SDs for each compound.

MTS assays. To evaluate cell viability, dimethylthiazol carboxymethoxyphenyl sulfophenyl tetrazolium (MTS) assays were performed using a Cell Titer 96 Aqueous One Solution cell proliferation assay (Promega) as previously reported (18, 22). Huh7/Rep-Feo cells and HCV-J6/JFH1-infected Huh7 cells were seeded in 96-well plates at a density of 8.0×10^3 cells/well. After treatment, to analyze the therapeutic index with the same concentration of the drug and administration time, 20 μl/well of Cell Titer 96 Aqueous One Solution reagent was added to the cells cultured in a 96-well plate, the plate was incubated at 37°C for 60 min, and then the absorbance at 490 nm was recorded with a 96-well plate reader. The cells were analyzed when the growth became confluent. Cell viability was expressed as the concentration required for 50% cytotoxicity (CC_{50}). The drug selectivity index was calculated as CC_{50}/EC_{50}. All experiments were performed in triplicate.

Analyses of drug synergism. The effects of treatment of Huh7/Rep-Feo cells with α-IFN, alone and in combination with TSN, were analyzed by using isobologram analysis as described previously (27, 37). Dose inhibition curves of α-IFN and TSN were drawn with the two drugs used alone or in combination. In each drug combination, EC_{50}s for α-IFN and TSN were plotted against the fractional concentration of α-IFN and TSN on the *x* and *y* axes, respectively. A theoretical line of additivity is drawn between plots of the EC_{50} for either drug that was used alone. The combined effects of the two drugs were considered additive, synergistic, or antagonistic if the plots of the drug combination were located on the line, below, or above the line of additivity, respectively.

HCV-J6/JFH1 cell culture. HCV-J6/JFH1 (21), which is a recombinant of HCV-JFH1 (42), was used. *In vitro*-synthesized HCV-J6/JFH1 RNA was transfected into naïve Huh7 cells (48), and the cells were cultured in the presence of drugs (34). Cellular viral RNA expression levels were measured using a real-time reverse transcription-PCR (RT-PCR) system.

Real-time RT-PCR analysis. Real-time RT-PCR was carried out as described previously (7). Total cellular RNA was extracted from cultured cells using Isogen (Nippon Gene, Tokyo, Japan), reverse transcribed, and subjected to real-time RT-PCR analyses. Expression of mRNA was quantified using TaqMan Universal PCR master mix, an ABI 7500 real-time PCR system (Applied Biosystems, CA), and a QuantiTect SYBR green PCR kit (Qiagen, CA). Some primers have been described elsewhere (30, 34). The primers used were -S (5'-TTT GAA ACA TCA AAG TTT TTC ACA GAC CTA-3'), -AS (5'-CAC AGT CAA GGT CCT TAG TAT TTC AGA TGT-3'), p56-S (5'-ACT TCG GAG AAA GGC ATT AGA TCT GGA AAG-3'), p56-AS (5'-TAA GGA CCT TGT CTC ACA GAG TTC TCA AAG-3'), Viperin-S (5'-GCT ACC AAG AGG AGA AAG CA-3'), Viperin-AS (5'-TTG ATC TTC TCC ATA CCA GC-3'), ISG20-S (5'-CTA CGA CAC GTC CAC TGA CAG G-3'), ISG20-AS (5'-CAT CGT TGC CCT CGC ATC TTC-3'), IRF9-S (5'-GCA GCA GCA GCC CTG AGC CAC AGG AAG TTA-3'), IRF9-AS (5'-TTA CCT GGA ACT TCG GTG GGG GGC CCA GGC-3'), IFNAR1-S (5'-CTT TCA AGT TCA GTG GCT CC-3'), IFNAR1-AS (5'-CAT CAG ATG CTT GTA CGC GGA G-3'), IFNAR2-S (5'-GCC AGA ATG CCT TCA TCG TCA G-3'), and IFNAR2-AS (5'-GTG AGT TGG TAC AAT GGA GTG G-3').

Western blotting. Twenty micrograms of total cell lysate was separated by SDS-PAGE and blotted onto a polyvinylidene fluoride Western blotting membrane. The membrane was incubated with the primary antibodies, followed by incubation with a peroxidase-labeled anti-IgG antibody, and were visualized by chemiluminescence using an enhance chemiluminescence Western blotting analysis system (Amersham Biosciences, Buckinghamshire, United Kingdom). The antibodies used were mouse anti-NS5A (BioDesign, ME), rabbit anti-signal transducer and activator of transcription 1 (anti-STAT1) p84/p91, rabbit anti-phospho-STAT1 (Tyr 701), rabbit anti-STAT2, rabbit anti-phospho-STAT2 (Tyr 690) (Santa Cruz, CA), and anti-beta-actin antibody (Sigma). NIH image software was used to analyze the densitometry of the Western blot analysis. Quantification of STAT phosphorylation was done using NIH image software, and the results correspond to the ratio between the phosphorylated STAT1 (p-STAT1) or p-STAT2 amount and the STAT1 or STAT2 amount normalized to the amount for the control without α-IFN and TSN. The results correspond to the ratio between the NS5A amount and the beta-actin amount normalized to the amount for the control without α-IFN and TSN.

Statistical analyses. Statistical analyses were performed using Student's *t* test. *P* values of less than 0.05 were considered statistically significant.

RESULTS

ISRE reporter screening. At the primary screening (n = 1), we defined a 1.5-fold induction in response to α-IFN to be a hit compound, and the hit rate was about 1%. At the secondary screening (n = 4), we selected the compound whose cps were 2 SDs larger than that for the drug used as a negative control, and the hit compound rate was 0.2% of the original library. Both assays were highly reproducible, and reflecting this, the Z' factor (46) for the ISRE reporter screen was 0.97.

TSN has activity against HCV RNA replication. Huh7/Rep-Feo cells were cultured with various concentrations of TSN, and the effect was measured using a luciferase assay. TSN caused a marked suppression of HCV RNA replication in a dose-dependent manner (Fig. 2A). The EC_{50} of TSN was 20.6 nM. In contrast, MTS assays showed that treatment with TSN had little effect on cellular viability and replication, with a CC_{50} of over 3 μM and a selectivity index of more than 146. These results indicated that TSN had an effect against HCV RNA replication when it was used alone and that the effect was specific for HCV replication and not attributable to nonspecific cytotoxicity (Fig. 2B). Similarly, by Western blotting (Fig. 2C), the expression of HCV NS5A protein was shown to be reduced by corresponding amounts following treatment with TSN. To determine whether TSN suppresses HCV IRES-dependent translation, we used a Huh7 cell line that had been stably transfected with pCIneo-Rluc-IRES-Fluc (Fig. 2D). Treatment of these cells with TSN resulted in no significant change of the internal luciferase activities at concentrations of TSN that suppressed expression of the HCV replicon.

TSN increased ISRE reporter activity with α-IFN. Because we identified TSN originally through ISRE reporter-based drug screening, we analyzed the effects of TSN on the cellular responses to α-IFN following pretreatment with TSN. First, we treated ISRE-TA-Luc-transfected Huh7 cells with TSN and α-IFN simultaneously or pretreated the cells with 10 to 100 nM TSN at 24 or 48 h prior to α-IFN treatment. Luciferase assays were performed 6 h after addition of α-IFN at concentrations of 0.1 to 100 IU/ml (Fig. 3A and B). Treatment with TSN alone did not increase ISRE reporter activity. Similarly, simultaneous treatment with TSN and α-IFN did not enhance α-IFN-induced ISRE reporter activation more than treatment with α-IFN alone. In contrast, pretreatment with TSN 24 or 48 h before addition of α-IFN significantly increased ISRE activation compared to that achieved by treatment with α-IFN alone (Fig. 3A). On the basis of these results, we performed the subsequent experiments with addition of TSN 24 h before α-IFN treatment.

We next quantified the expression levels of ISGs, including those for 2′,5′-oligoadenylate synthetase (25AS), MxA, protein kinase R, p56, viperin, and ISG20, which encode proteins with direct antiviral activity (14, 15, 25). Naïve Huh7 cells were treated with TSN for 24 h, followed by treatment with 100 IU/ml α-IFN for 24 h. The expression of each ISG was significantly elevated in a dose-dependent manner following pretreatment with TSN and α-IFN stimulation (Fig. 3C). These results indicated that TSN pretreatment significantly enhanced the cellular response to α-IFN-induced, ISRE-regulated expression of ISGs.

It has been reported that α-IFN receptor-mediated signaling

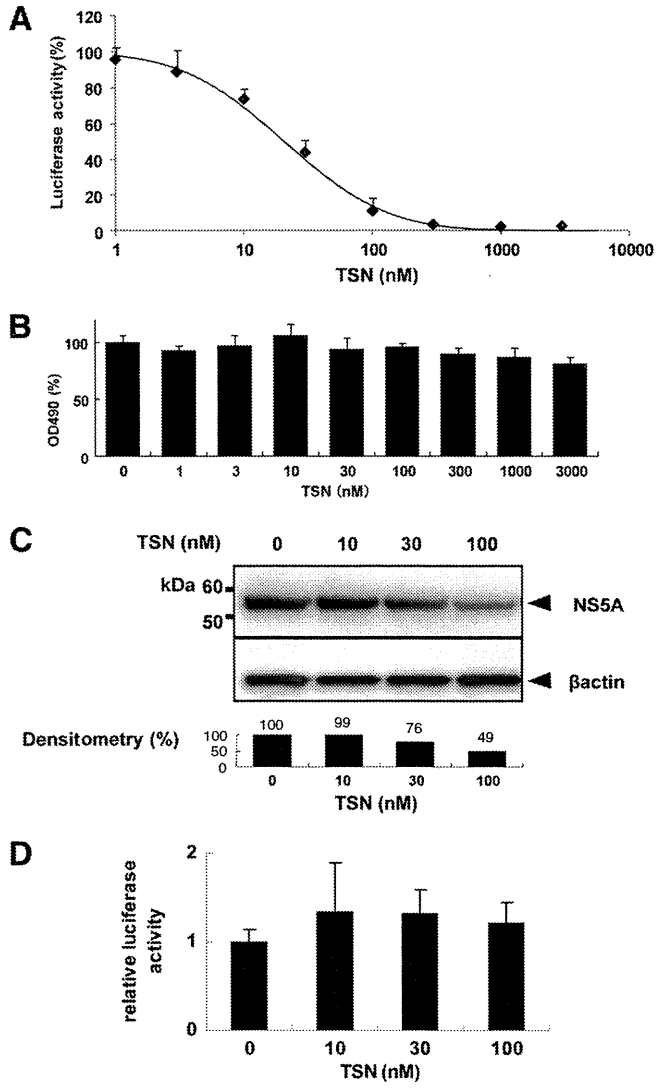

FIG. 2. Effect of TSN on expression of HCV replicon. (A) HCV replicon cells were treated with various concentrations of TSN for 48 h. Replication levels of HCV RNA were analyzed by luciferase assay. Bars indicate luciferase activities relative to that of the drug-negative control. (B) Cell viability was determined by MTS assay. Bars indicate the value relative to that of the drug-negative control. (C) Western blotting analyses. The expression of NS5A and beta-actin was detected using anti-NS5A and anti-beta-actin antibodies. Densitometry of NS5A protein was performed, and the result is indicated as a percentage of the result for the drug-negative control. The assay was repeated three times, and a representative result is shown. (D) A bicistronic reporter gene plasmid, pCIneo-Rluc-IRES-Fluc, was transfected into Huh7 cells. The cells were cultured with TSN at the concentrations indicated, and dual luciferase activities were measured after 24 h of treatment. Values are displayed as ratios of Fluc to Rluc. In panels A, B, and D, the assays were done in triplicate and repeated three times. Error bars indicate means ± SDs.

cross talks with several alternative pathways, including the NF-kappaB, gamma IFN, phosphatidylinositol 3-kinase (PI3K), and mitogen-activated protein kinase (MAPK) pathways (9, 16, 24, 28). Therefore, we analyzed the effect of TSN on the signaling pathways indicated above. Cells were transfected with various reporter plasmids, including NF-kappaB, gamma